


 Cite this: *RSC Adv.*, 2025, 15, 33162

# Multifunctional transition metal oxide/graphene oxide nanocomposites for catalytic dye degradation, renewable energy, and energy storage applications

Viraj Pasindu, Piumika Yapa, Sanduni Dabare and Imalka Munaweera \*

The worsening global environmental and energy crises involving industrial water pollution, carbon emissions and clean, sustainable energy requirements call for innovative multifunctional materials. Transition metal oxide/graphene oxide (TMO/GO) nanocomposites represent an advanced material group through their ability to integrate redox properties of transition metal oxides and catalytic characteristics with graphene derivative characteristics, which include electrical conductivity, low surface area, and exceptional mechanical strength. While TMO/GO composites demonstrate promising multifunctional abilities in dye degradation, energy storage, and renewable energy applications, critical challenges remain unaddressed. First, scalable synthesis methods for defect-free graphene hybrids with uniform TMO nanoparticle distribution are underdeveloped, as current solvothermal or sol-gel approaches often yield inconsistent morphologies and require surfactants or toxic solvents. Second, the long-term stability of these composites under operational conditions remains poorly characterized, with limited studies on mechanical degradation or leaching of toxic metal ions. Third, while individual functionalities (photocatalysis, capacitance) are well-studied, synergistic optimization of dual/multifunctional performance is largely unexplored. This review gives a thorough examination of synthesis methods (sol-gel and hydrothermal) and metal doping protocols for surface functionalization and TMO/GO composite behavior related to their unique applications. This review gives a thorough examination of synthesis methods (sol-gel and hydrothermal) and metal doping protocols for surface functionalization and TMO/GO composite behavior related to their unique applications. The paper evaluates existing research gaps and sustainability factors by delivering an analytical assessment of the scalability as well as durability, and sustainable development applicability across next-generation clean water technologies and renewable energy conversion and energy storage systems.

 Received 5th July 2025  
 Accepted 23rd August 2025

DOI: 10.1039/d5ra04806k

[rsc.li/rsc-advances](https://rsc.li/rsc-advances)

## 1. Introduction

The development of innovative materials with multiple functions occurs because of escalating international requirements for clean energy storage while requiring rapid solutions to eliminate environmental pollutants particularly those found in water systems.<sup>1</sup> Transition metal oxides (TMOs) are widely employed in photocatalysis and energy storage owing to their capacity to easily modify their oxidation states, participate in redox processes, and exhibit semiconducting properties. These characteristics make them exceptionally effective in degrading contaminants like dyes and in accumulating electrical energy. Benchmark metal oxides, including zinc oxide (ZnO), nickel oxide (NiO), cobalt oxide (CoO<sub>4</sub>), and titanium dioxide (TiO<sub>2</sub>),

have been extensively studied for their inherent benefits in photocatalysis, energy storage, and environmental remediation. Despite its wide bandgap (3.37 eV), significant exciton binding energy, and cost-effectiveness, ZnO's practical applicability is constrained by low electrical conductivity, a high rate of charge recombination, and photodegradation under UV irradiation. Likewise, NiO, esteemed for its electrochemical stability and p-type conductivity, has reduced light absorption, diminished intrinsic conductivity, and particle aggregation. Cobalt oxide (Co<sub>3</sub>O<sub>4</sub>) exhibits mixed valence states (Co<sup>2+</sup>/Co<sup>3+</sup>) and exceptional catalytic efficacy, rendering it attractive for oxygen evolution and supercapacitor applications; however, its low electronic conductivity, propensity for nanoparticle agglomeration, and stability concerns under extreme conditions present considerable challenges. TiO<sub>2</sub>, arguably the most extensively studied oxide, is celebrated for its exceptional photocatalytic efficiency, high durability, and non-toxic characteristics; however, its wide bandgap (~3.2 eV) restricts visible light

Department of Chemistry, Faculty of Applied Sciences, University of Sri Jayawardenepura, Nugegoda 10250, Sri Lanka. E-mail: [pasinduviraj8@gmail.com](mailto:pasinduviraj8@gmail.com); [piumikayapa@gmail.com](mailto:piumikayapa@gmail.com); [dabaresanduni@gmail.com](mailto:dabaresanduni@gmail.com); [imalka@sjp.ac.lk](mailto:imalka@sjp.ac.lk)



Table 1 A study on properties of TMO systems

TMO system	Tunable oxidation states	Redox activity	Semiconducting behavior	Corresponding research article
Fe-doped $\text{Co}_3\text{O}_4$	$\text{Co}^{2+}/\text{Co}^{3+}$ and $\text{Fe}^{3+}$ states enable dynamic redox shifts	Enhanced pseudo capacitance ( $588.5 \text{ F g}^{-1}$ ) via $\text{Co}^{2+}/\text{Co}^{3+}$ and $\text{Fe}^{3+}$ redox couples	Bandgap reduction to 2.0 eV (vs. 2.96 eV in pure $\text{Co}_3\text{O}_4$ ), improving visible-light absorption	Synergistic photocatalytic and super capacitive properties of transition metal doped $\text{Co}_3\text{O}_4$ : towards efficient dye degradation and energy storage ( <i>SSRN</i> , 2024) <sup>5</sup>
$\text{MnO}_2$	$\text{Mn}^{3+}/\text{Mn}^{4+}$ transitions facilitated by oxygen vacancies	Pseudocapacitive charge storage via reversible Mn redox reactions	Dielectric properties enable dual functionality as separator and electrode	Photoinduced simultaneous thermal and photocatalytic activities of $\text{MnO}_2$ revealed by femtosecond transient absorption spectroscopy ( <i>ACS Appl. Mater. Interfaces</i> , 2021)
Ni-doped $\text{V}_2\text{O}_5$	$\text{V}^{4+}/\text{V}^{5+}$ shifts enhanced by Ni doping and O-vacancies	High specific capacity ( $3485 \text{ F g}^{-1}$ at $1 \text{ A g}^{-1}$ ) from enriched redox sites	Improved electrical conductivity via optimized oxygen deficiency	Exploration of oxygen-deficiencies coupled with Ni-doped $\text{V}_2\text{O}_5$ nanosheets ( <i>SSRN</i> , 2023)
$\text{RuO}_2$	Reversible $\text{Ru}^{4+}/\text{Ru}^{3+}/\text{Ru}^{2+}$ transitions	Quasi-rectangular CV curves from reversible redox processes	Low resistivity and high thermal stability	Graphene nanosheet-supported ultrafine $\text{RuO}_2$ quantum dots as electrochemical energy materials ( <i>SSRN</i> )
$\text{CuO}/\text{SnO}_2$	$\text{Cu}^+/\text{Cu}^{2+}$ and $\text{Sn}^{4+}$ states in heterojunctions	Enhanced redox kinetics at p-n interfaces	Bandgap $\sim 2.1$ – $2.6$ eV, improved charge separation	Photocatalytic degradation and electrochemical energy storage properties of $\text{CuO}/\text{SnO}_2$ nanocomposites via the wet-chemical method ( <i>Chemosphere</i> , 2023)
$\text{CeO}_2$ - $\text{SnO}_2$	$\text{Ce}^{3+}/\text{Ce}^{4+}$ and $\text{Sn}^{4+}$ redox couples	Efficient electron-hole separation at heterojunctions	Bandgap reduction via composite formation	Efficient photocatalytic, antibacterial, and energy storage properties of $\text{CeO}_2$ - $\text{SnO}_2$ composite nanofibers ( <i>Nanomaterials</i> , 2023)
$\text{SnO}_2$	$\text{Sn}^{4+}$ with oxygen-vacancy-mediated states	Surface-dependent redox activity	UV-driven photocatalysis with tunable bandgap	Effect of calcination temperature and pressure-assisted heat treatment on the dye degradation performance of $\text{SnO}_2$ photocatalyst ( <i>Mater. Res. Bull.</i> , 2022)
CTAB-modified $\text{CuO}$	$\text{Cu}^{2+}$ with surfactant-enhanced surface states	Improved charge transfer kinetics	Bandgap $\sim 1.7$ eV, visible-light responsive	Surface-modified $\text{CuO}$ nanoparticles for photocatalysis and highly efficient energy storage devices ( <i>PubMed</i> , 2023)

absorption, and its application is additionally impeded by rapid charge carrier recombination and inadequate conductivity. The acknowledged constraints highlight the pressing necessity for material improvements, including doping, heterostructure engineering, and nano structuring, to boost the functional performance of these benchmark systems.

TiO<sub>2</sub> and ZnO dominate UV-driven photocatalysis, leveraging high oxidative potentials to degrade dyes such as methylene blue and rhodamine B through hydroxyl radical generation.<sup>2</sup> Similarly, Co<sub>3</sub>O<sub>4</sub> and NiO excel in supercapacitors and battery electrodes, where multiple oxidation states (*e.g.*, Co<sup>2+</sup>/Co<sup>3+</sup>) enable high pseudo capacitance. However, intrinsic limitations persist, including rapid charge recombination in TiO<sub>2</sub> (reducing photocatalytic efficiency), poor electrical conductivity in NiO/Co<sub>3</sub>O<sub>4</sub> (limiting charge transfer), and particle agglomeration during synthesis (diminishing active surface area).<sup>3,4</sup> To address these limitations, researchers have developed heterostructure TMO composites, in which Fe-doped Co<sub>3</sub>O<sub>4</sub> decreases bandgaps to around 2.0 eV, thus improving visible-light absorption for dye degradation. Furthermore, Co<sub>3</sub>O<sub>4</sub>-coated TiO<sub>2</sub> core-shell structures establish p-n junctions that improve charge separation and increase photocatalytic effectiveness, attaining nearly 100% degradation of methylene blue in about 1.5 hours under UV light, compared to 80% for uncoated TiO<sub>2</sub>. Moreover, CuMn bimetallic oxides create conductive networks that mitigate volume expansion in lithium-ion batteries, as demonstrated by hierarchically porous MnO-rich CuMn oxide anodes featuring *in situ* generated Cu conductive networks, which exhibit high areal capacity and stability over numerous cycles.

Multifunctionality of transition metal oxide (TMO) systems in photocatalytic dye degradation and energy storage applications, Table 1 summarizes key examples that highlight the interplay between their redox-active centers, tunable oxidation states, and semiconducting behavior. These materials not only exhibit enhanced charge-transfer dynamics and visible-light responsiveness but also demonstrate impressive performance metrics in both photocatalytic and super capacitive domains. The selected studies underscore how doping strategies, oxygen vacancies, and heterojunction engineering collectively modulate electronic structure and surface chemistry thereby bridging

the gap between environmental remediation and sustainable energy technologies.

TMOs like Fe-doped Co<sub>3</sub>O<sub>4</sub> and CuO/SnO<sub>2</sub> heterojunctions leverage tunable bandgaps (*e.g.*, 2.0 eV) and redox-active sites to simultaneously drive photocatalytic pollutant breakdown and high-capacity energy storage. These dual-function systems exemplify how oxygen vacancies and heterojunction engineering previously shown to enhance charge separation in dye degradation directly enable scalable renewable energy applications. For instance, hierarchical CuMn oxides mitigate volume expansion in batteries, while RuO<sub>2</sub>/graphene hybrids achieve record pseudo capacitance (523 F g<sup>-1</sup>), directly extending the charge-transfer dynamics discussed in photocatalytic contexts. Such innovations demonstrate TMOs' unique capacity to bridge environmental remediation and energy sustainability, fulfilling global demands for integrated clean technology solutions. A comparative analysis of recent supercapacitor materials shows the progress in enhancing both specific capacitance and long-term cyclic retention as studied in Table 1. For instance, *N*-butyllithium-treated Ti<sub>3</sub>C<sub>2</sub>T<sub>x</sub> MXene demonstrated a high specific capacitance of 523 F g<sup>-1</sup> at 2 mV s<sup>-1</sup> and excellent cyclic retention of 96% after 10 000 cycles, highlighting the efficiency of surface functionalization (Chen *et al.*, 2019).<sup>6</sup> Similarly, Li<sub>4</sub>Ti<sub>5</sub>O<sub>12</sub> modified with MgCl<sub>2</sub> electrolyte additive displayed improved initial discharge capacities of 290 mA h g<sup>-1</sup>, with almost 99.9% capacity retention by the 40th cycle and moderate rate-dependent performance (Cabello *et al.*, 2019).<sup>7</sup> In another study, WO<sub>3</sub>·0.5H<sub>2</sub>O nanoparticles decorated on reduced graphene oxide (rGO) achieved capacitance values ranging from 241 to 306 F g<sup>-1</sup>, depending on Ni<sup>2+</sup> adsorption, and showed good long-term stability—up to 90% retention after 10 000 cycles and 75–82% after 12 000 cycles (Mashkoo *et al.*, 2023).<sup>8</sup> These studies collectively emphasize the role of surface modification, composite structuring, and electrolyte engineering in advancing supercapacitor electrode performance.

While the data in Table 2 above highlights key performance indicators such as specific capacitance and cycling stability for various electrode systems, another equally important metric, Coulombic Efficiency (CE), which the above studies haven't mentioned. Several studies have reported CE to evaluate the electrochemical stability and reversibility of advanced electrode

**Table 2** Comparison of pseudo capacitor performance metrics of selected electrode materials, highlighting specific capacitance and cycling stability

Paper	Material/System	Specific capacitance (F g <sup>-1</sup> or mA h g <sup>-1</sup> )	Cyclic retention/stability
<i>N</i> -Butyllithium treated Ti <sub>3</sub> C <sub>2</sub> T <sub>x</sub> MXene with excellent pseudo capacitor performance (Chen <i>et al.</i> , 2019) <sup>11</sup>	<i>N</i> -Butyllithium-treated Ti <sub>3</sub> C <sub>2</sub> T <sub>x</sub> MXene	523 F g <sup>-1</sup>	96% after 10 000 cycles
On the beneficial effect of MgCl <sub>2</sub> as electrolyte additive to improve the electrochemical performance of Li <sub>4</sub> Ti <sub>5</sub> O <sub>12</sub> (Cabello <i>et al.</i> , 2019) <sup>7</sup>	Li <sub>4</sub> Ti <sub>5</sub> O <sub>12</sub> with MgCl <sub>2</sub> additive (Mg battery cathode)	290 mA h g <sup>-1</sup> (initial discharge) ~175 mA h g <sup>-1</sup> theoretical	99.9% retention at 40th cycle
Synergistic effects of WO <sub>3</sub> ·0.5H <sub>2</sub> O-rGO for supercapacitors (Mashkoo <i>et al.</i> , 2023) <sup>8</sup>	WO <sub>3</sub> ·0.5H <sub>2</sub> O: 306.42 F per g rGO-WO	90% after 10 000 cycles 75% after 12 000 cycles 82% after 14 000 cycles	Not specified



materials. For instance, Yun *et al.* (2015) investigated MnO<sub>2</sub>-coated carbon materials and observed a high CE of ~98% over 5000 cycles, attributing it to the stable redox reactions of Mn<sup>4+</sup>/Mn<sup>3+</sup>.<sup>9</sup> Similarly, Xia *et al.* (2017) examined layered double hydroxide (LDH)-based supercapacitors and noted CE consistently above 95%, suggesting high cycling reversibility.<sup>10</sup> Chen *et al.* (2019),<sup>6</sup> while focusing on Ti<sub>3</sub>C<sub>2</sub>T<sub>x</sub> MXene for supercapacitors, reported high cycling stability but did not explicitly report CE; however, other MXene-based systems often show CE in the range of 90–99%, depending on surface termination and electrolyte compatibility. In pseudocapacitive systems involving metal oxides or composites (*e.g.*, NiCo<sub>2</sub>O<sub>4</sub>, WO<sub>3</sub>, or rGO hybrids), CE typically remains above 90%, provided proper electrode–electrolyte interfaces and stable redox couples are maintained.

Although high CE is a strong indicator of electrochemical reversibility and material stability, achieving simultaneously high capacitance, stability, and efficiency remains challenging, especially in single-component systems. To overcome these limitations, composite nanomaterials, particularly those combining transition metal oxides (TMOs) with graphene derivatives have emerged as highly promising candidates for next-generation energy storage devices.<sup>12</sup> These TMO/graphene oxide (TMO/GO) composites synergistically integrate the redox activity and semiconducting properties of TMOs such as ZnO, TiO<sub>2</sub>, and NiO with the exceptional electrical conductivity, high surface area, and mechanical flexibility of graphene-based materials like GO and rGO. As a result, they offer enhanced physicochemical interactions, improved charge transport, and suppressed agglomeration ultimately enabling electrochemical performances that exceed those of the individual components.

## 2. Transition metal oxides: synthesis and functionalization

Transition metals, occupying groups from 3 to 12 of the periodic table, possess partially filled d-orbitals, that enable them to exhibit variable oxidation states, high electronic conductivity, and catalytic activity. These unique features make them central to numerous techno-industrial applications, including energy storage, catalysis, and environmental remediation. Transition metal oxides (TMOs), such as ZnO, TiO<sub>2</sub>, and Co<sub>3</sub>O<sub>4</sub>, are typically synthesized through methods like sol–gel, hydrothermal, and co-precipitation techniques. Among these, the sol–gel method offers superior control over particle size, morphology, and surface area, making it particularly well-suited for producing high-surface-area, reactive nanostructured TMOs ideal for advanced functional applications.<sup>13,14</sup> In recent years, the sol–gel method has been extensively utilized for the advancement of innovative oxide nanostructures and useful materials. A significant trend is the increasing emphasis on producing low-dimensional metal oxide nanostructures, including nanoparticles, nanorods, and nanosheets, by sol–gel methods. This method's inherent versatility and precise control renders it exceptionally suitable for customizing the structural, morphological, and surface properties of nanostructures, which

are essential for improving their performance in applications such as photocatalysis, energy storage, and environmental remediation. High-surface-area structures are particularly examined for gas sensors and catalysts, since their diminutive size and porosity improve performance. A significant emphasis in sol–gel research is the advancement of templated or porous materials. This method involves the incorporation of surfactants or sacrificial templates during the sol stage to guide the synthesis of periodic mesoporous metal oxides, including mesoporous silica, alumina, or mixed-oxide frameworks. These templated sol–gel methods are widely documented for producing high-surface-area catalytic supports, which provide increased accessibility to active sites and enhanced mass transport characteristics. Hydrothermal synthesis is a commonly utilized method for the fabrication of transition metal oxides (TMOs), providing an efficient pathway to highly crystalline and precisely defined nanostructures. This technique entails the chemical reaction of precursors within a sealed autoclave at elevated temperature and pressure, generally in an aqueous environment. The regulated conditions promote the development of various TMO morphologies, such as nanorods, nanowires, nanotubes, and hierarchical structures, often with limited agglomeration. Hydrothermal synthesis is widely employed for the production of transition metal oxides (TMOs) such as TiO<sub>2</sub>, ZnO, Co<sub>3</sub>O<sub>4</sub>, and Fe<sub>3</sub>O<sub>4</sub>, owing to its simplicity, scalability, and capability to customize particle size and crystallinity, especially for applications in photocatalysis, energy storage, and environmental remediation.

Hydrothermal-synthesized TMOs are key in energy and environmental fields. For example, hierarchical composite electrodes (NiCo<sub>2</sub>O<sub>4</sub>@MnMoO<sub>4</sub> on Ni foam) have been prepared *via* multi-step hydrothermal routes, achieving very high supercapacitor capacitances.<sup>15</sup> Similarly, hybrid 2D/oxide materials (*e.g.* Ti<sub>3</sub>C<sub>2</sub>T<sub>x</sub> MXene decorated *in situ* with CuS nanoparticles and carbon dots by hydrothermal treatment) show excellent battery electrode performance.<sup>16</sup> In photovoltaics and photocatalysis, researchers exploit hydrothermal morphology control to optimize light absorption and surface reaction sites. Overall, current hydrothermal research emphasizes precise shape control (rods, plates, hollow spheres), green solvents (water-only systems), and integration with substrates or composites for functional devices.

Transmission Electron Microscopy (TEM) is an advanced characterization method for examining the morphology and microstructure of transition metal oxides (TMOs) at the nano-scale. TEM offers high-resolution images that disclose intricate details regarding particle morphology, size distribution, crystalline, and surface characteristics. TEM examination enables the direct visualization of many TMO nanostructures, including nanoparticles, nanorods, nanosheets, and hollow or core–shell morphologies. Additionally, Selected Area Electron Diffraction (SAED) patterns acquired during Transmission Electron Microscopy (TEM) investigation corroborate the crystalline characteristics and phase purity of the produced transition metal oxides (TMOs). This degree of morphological expertise is essential for comprehending structure–property correlations in transition metal oxides, particularly for enhancing their efficacy





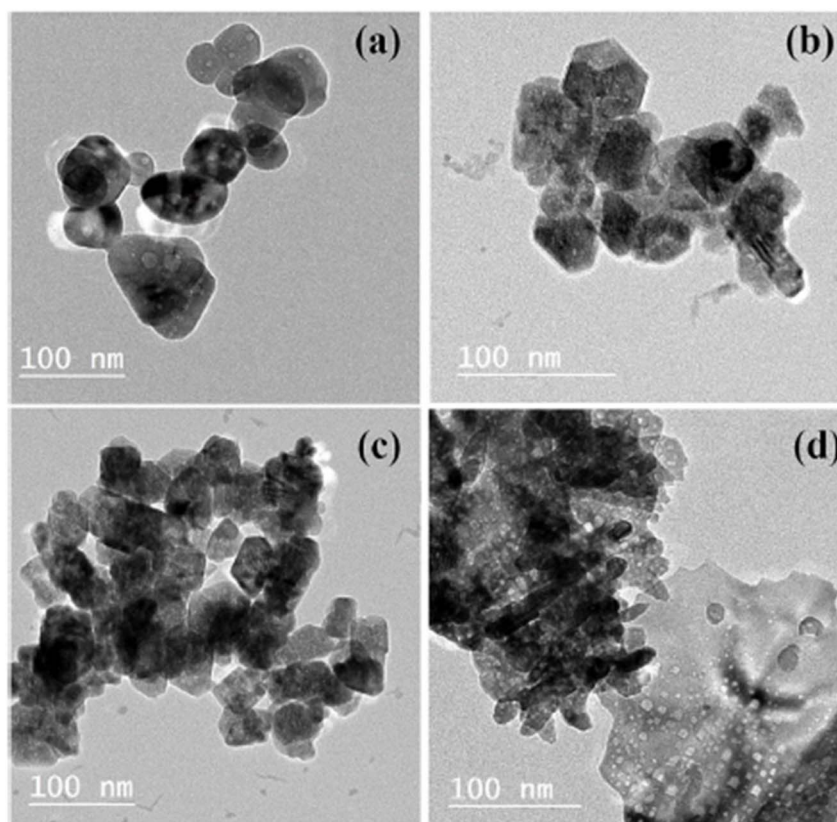


Fig. 1 TEM images of (a) undoped ZnO (b) Mg/ZnO (c) Cu/ZnO (d) Sn/ZnO. (Reproduced from ref. 18 with permission from Springer Nature, copyright 2023).

in photocatalytic, energy storage, and environmental applications. Fig. 1 depicts the TEM images of undoped ZnO, Mg/ZnO, Cu/ZnO, and Sn/ZnO. Fig. 1 presents TEM images of four different ZnO-based nanomaterials: (a) undoped ZnO, (b) Mg-doped ZnO, (c) Cu-doped ZnO, and (d) Sn-doped ZnO. Each panel shows distinct nanoparticle morphologies at the same scale (100 nm). The undoped ZnO (a) displays relatively large, somewhat spherical or irregularly shaped particles. When doped with Mg (b), the particles appear more faceted and smaller, indicating that Mg incorporation influences crystal growth, often resulting in reduced grain size and more defined shapes. Cu-doped ZnO (c) shows further aggregation and a more compact arrangement of smaller particles, suggesting that Cu doping can enhance nucleation and lead to dense nanostructures. The Sn-doped ZnO (d) exhibits a highly dense cluster of even smaller nanoparticles, with a uniform distribution, which is consistent with reports that Sn doping can significantly alter the morphology and increase the density of ZnO nanostructures. These morphological changes upon doping are important, as they can directly affect the optical, electrical, and catalytic properties of ZnO materials.<sup>17</sup>

Phase analysis of transition metal oxides (TMOs) is routinely performed using Powder X-ray Diffraction (PXRD), a non-destructive, reliable technique for identifying crystalline phases and assessing structural purity. PXRD provides characteristic diffraction patterns based on the crystal structure, allowing accurate determination of phase composition, crystallite size,

and degree of crystalline. Additionally, PXRD can reveal secondary or impurity phases, which is crucial for ensuring the structural and functional integrity of nanomaterials intended for applications like photocatalysis, energy storage, and environmental remediation. Fig. 2 illustrates PXRD data for undoped ZnO, Mg/ZnO, Cu/ZnO, and Sn/ZnO. Fig. 2 shows PXRD (Powder X-ray Diffraction) patterns for undoped ZnO and ZnO doped with Mg, Cu, and Sn. In panel (a), the diffraction peaks for all samples (I: ZnO, II: Mg/ZnO, III: Cu/ZnO, IV: Sn/ZnO) are indexed to the hexagonal wurtzite structure of ZnO, with prominent peaks at planes (100), (002), (101), and others. The similarity in peak positions across all samples indicates that doping with Mg, Cu, or Sn does not alter the fundamental crystal structure of ZnO. Panel (b) provides a magnified view of the main peaks, showing that the intensity and sharpness of the peaks remain consistent, suggesting that the dopants are well incorporated without forming secondary phases. Minor shifts in peak positions may be observed, reflecting slight lattice distortions due to the substitution of Zn ions with dopant ions of different sizes, but the overall phase purity and crystallinity of ZnO are preserved in all doped samples.<sup>17</sup>

The functionalization of transition metal oxides (TMOs) is essential for modifying their electronic structure and decreasing their band gap into the ultraviolet-visible spectrum, facilitating their application in photocatalysis, optoelectronics, and solar energy conversion. Doping has emerged as the most promising functionalization strategy due to its capacity to



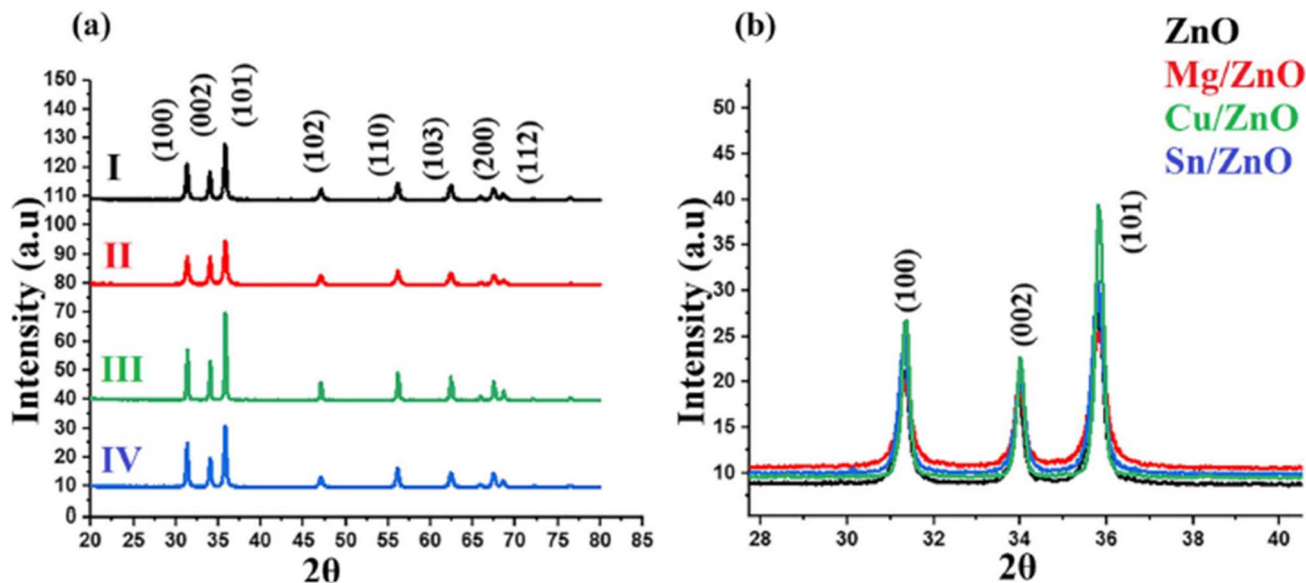


Fig. 2 (a) XRD patterns of (I) undoped ZnO (II) Mg/ZnO (III) Cu/ZnO (IV) Sn/ZnO. (b) High-resolution XRD patterns of undoped and doped ZnO NPs. (Reproduced from ref. 17 with permission from Springer, copyright 2024).

precisely alter the band structure by integrating foreign atoms into the TMO lattice. This introduces supplementary energy levels, augments visible-light absorption, and promotes charge separation efficiency. Doping provides superior scalability and tunability compared to techniques like morphological tuning or surface engineering, rendering it especially advantageous for the progression of TMO-based technologies in scientific research and industrial applications.

Doping transition metal oxides (TMOs) such as ZnO, TiO<sub>2</sub>, and Co<sub>3</sub>O<sub>4</sub> significantly alters their band gap energies, thereby enhancing their multifunctionality in photocatalytic dye

degradation and energy storage. For example, undoped ZnO typically has a band gap of about 3.23 eV, but doping with transition metals like Fe, Mn, or Co can increase this value to around 3.33 eV, while other dopants such as Cu or Mg may introduce intermediate energy levels that effectively narrow the band gap, improving visible-light absorption. Similarly, TiO<sub>2</sub>'s band gap can be reduced from ~3.2 eV in its pure form to a range of 2.20–2.48 eV when doped with metals like Mn, Co, Ni, or Mo, and Fe doping in Co<sub>3</sub>O<sub>4</sub> can lower the band gap to about 2.0 eV. These changes in electronic structure, achieved more precisely and scalable through doping than by morphological or surface modifications, enhance

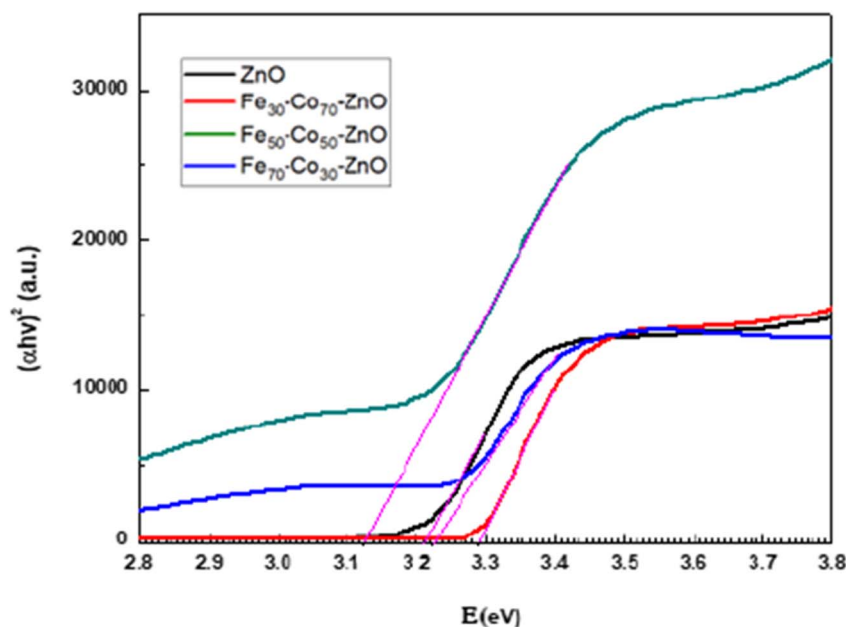


Fig. 3 Tauc plots for pure ZnO and doped ZnO samples used to calculate the band gap. (Reproduced from ref. 19 with permission from MDPI, copyright 2022).

charge separation efficiency and broaden the absorption spectrum, directly contributing to improved photocatalytic and energy storage performance in TMO-based systems.

The attached Fig. 3 illustrates the effect of Fe and Co doping on the optical band gap of ZnO, as determined by Tauc plot analysis. The plot shows  $(\alpha h\nu)^2$  versus photon energy ( $E$ ) for undoped ZnO and for ZnO doped with varying Fe and Co ratios. The undoped ZnO (black curve) exhibits an absorption edge corresponding to a band gap near 3.2 eV. As the Fe and Co content increases (moving from Fe<sub>30</sub>Co<sub>70</sub>-ZnO to Fe<sub>70</sub>Co<sub>30</sub>-ZnO), the absorption edge shifts to higher energies, indicating a widening of the band gap. This trend confirms that certain transition metal dopants can increase the band gap of ZnO, as seen by the rightward shift of the curves. The ability to tune the band gap through controlled doping is critical for optimizing the material's optical and electronic properties for specific photocatalytic and energy storage applications.

### 3. Transition metal oxide/graphene oxide nanocomposites

Graphene oxide (GO) is a two-dimensional carbon scaffold rich in oxygen functional groups, while transition metal oxides (TMOs) (e.g. TiO<sub>2</sub>, Co<sub>3</sub>O<sub>4</sub>, Fe<sub>2</sub>O<sub>3</sub>) provide redox-active sites. When integrated at the material level, GO-TMO hybrids exhibit strong interfacial bonding and heterojunction effects. Chemical bonding typically involves coordination or covalent interactions between TMO metal centers and GO's oxygen groups (epoxies, hydroxyls, carboxyls). For example, depositing metal oxides on graphene induces C-O-M linkages: aluminum oxide on graphene forms sp<sup>3</sup> C-O bonds at the interface.<sup>16</sup> Such bonding can create interface defects and charge-transfer. In AlO<sub>x</sub>/graphene, interfacial sp<sup>3</sup> C-O bonds induce strong p-type doping. Similarly, GO-Co<sub>3</sub>O<sub>4</sub> hybrids form covalent bonds: theory shows Co<sub>3</sub>O<sub>4</sub> nanocubes bind to GO and "etch" surface oxygen, creating two Co-C bonds and driving  $\approx 2.25e$  of charge transfer.<sup>20</sup> In essence, GO's oxide groups chemisorb TMOs, altering GO's chemistry and creating defect sites (sp<sup>3</sup> C-O bonds, vacancies) that govern interface electronic structure.

GO-TMO interfaces also form heterojunctions that align energy bands. Many TMOs are semiconductors (bandgaps 2–4 eV) and GO (or its reduced form rGO) is a narrow-gap carbon material, so a p-n or type-II junction often arises. For instance, ultrathin MoO<sub>3</sub> on CVD graphene creates a large interface dipole and band bending: MoO<sub>3</sub> (an n-type oxide) contacts graphene, causing  $\sim 1.9$  eV band-offset and strong p-doping of graphene (Fermi level shifts by  $\sim 0.25$  eV).<sup>21</sup> This effect aligns the transport levels for efficient charge flow. Similarly, Cu<sub>2</sub>O-CoO nanoparticles on GO form complex heterojunctions: CoO and Cu<sub>2</sub>O have complementary band edges, and when integrated with GO they produce mixed-valence states that improve charge extraction.<sup>22</sup> In general, layered GO-TMO hybrids facilitate charge separation: photoexcited electrons localize in one component (e.g. GO) while holes remain in the oxide (or *vice versa*), reducing recombination. This is crucial in photocatalysis and photovoltaics. Indeed, GO-based heterostructures (e.g.

TiO<sub>2</sub>-GO, ZnO-GO) often show type-II behavior, though detailed band alignments depend on material and doping.

Transition metal oxide/graphene (TMO/GR) composites enhance energy storage and environmental applications through synergistic mechanisms. In lithium/sodium-ion batteries (LIBs/SIBs) and supercapacitors, graphene's porous structure facilitates efficient ion diffusion, while TMOs enable pseudocapacitive and faradaic reactions, boosting storage capacity and charge-discharge kinetics.<sup>13,23</sup> However, challenges like volume expansion in TMOs during cycling necessitate graphene's elastic matrix to buffer mechanical stress.<sup>14</sup> Supercapacitors benefit from graphene's electric double-layer capacitance and TMOs' redox activity, optimizing energy-power density trade-offs.<sup>15</sup> Despite these advantages, scaling lab-scale hydrothermal synthesis to cost-effective industrial production remains a barrier.<sup>14</sup> Eco-friendly synthesis methods using sustainable precursors and solvents are critical to minimizing environmental impacts, alongside rigorous life-cycle assessments to address nanoparticle toxicity and reuse limitations.<sup>16,18</sup> TMO/GR composites align with global sustainability goals by enabling water decontamination, renewable energy storage, and CO<sub>2</sub> to fuel conversion.<sup>21</sup> Their multifunctionality supports clean water access through photocatalytic degradation and advances decarbonized energy systems *via* high-performance electrodes.<sup>21,22</sup> However, commercial deployment requires overcoming technical hurdles, including stable thin-film fabrication, 3D-printed structure integration, and standardized durability testing.<sup>19,20</sup> Interdisciplinary research and supportive legislative frameworks are essential for transitioning these materials from laboratory investigations to viable, scalable solutions. TMO/GO composites, by combining environmental remediation with energy storage capabilities, exemplify a category of advanced materials poised to advance sustainable circular economies. To actualize this promise, it is essential that their synthesis, application, and end-of-life management adhere to ecologically sustainable principles, thereby ensuring technical progress alongside ecological accountability.<sup>22,24</sup>

Transition metal oxide/graphene oxide (TMO/GO) hybrids possess impressive properties through synergy of their intrinsic structural and electronic features. Interfacial charge transfer is essential due to the proper energy band alignment between TMOs and GO. This triggers high-speed electron mobility, reduces charge carrier recombination, and enhances overall conductivity, a property of great utility in both photocatalyst and electrochemical applications. GO plays a crucial role as an electron sink in TiO<sub>2</sub>/GO composites, capturing photoexcited electrons produced in TiO<sub>2</sub>. This capability significantly boosts the efficiency of photocatalytic processes, making these composites highly effective for various applications. The interplay of redox processes with transition metal oxides (TMOs) presents a powerful opportunity. TMOs, known for their multiple oxidation states, uniquely collaborate with defect sites and oxygen-functional groups in graphene oxide (GO), driving highly efficient redox cycling. This synergy is not just beneficial; it is foundational for advancing catalysis and energy storage technologies. Moreover, the exceptional high surface area and functionalization of GO create an outstanding framework that significantly boosts the





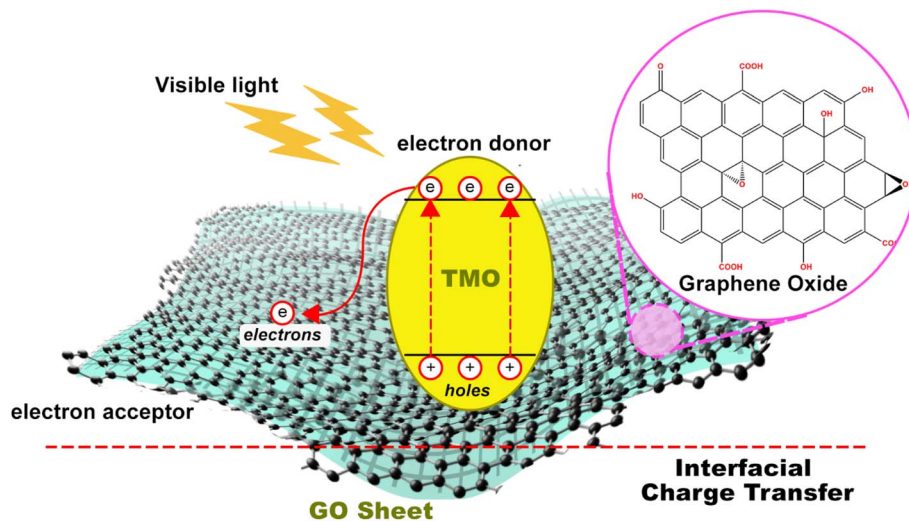


Fig. 4 Schematic diagram of the mechanisms of TMO/GO composites. (Authors' work).

dispersion and accessibility of TMO active sites, thereby enhancing ion diffusion as mentioned in Fig. 4.

Moreover, interface stability and electronic contact in the TMO/GO composites are aided by  $\pi$ - $\pi$  interaction, hydrogen bonding, and metal-oxygen-carbon bridging between the  $sp^2$  domains of GO and the TMO nanoparticles. The chemical and physical bonds in this hybrid architecture play a crucial role, not only reinforcing its stability but also enhancing the efficiency of electron transport throughout the system. Bandgap modulation seems to be another key mechanism, reduced GO morphs can alter the electronic structure of TMOs, optimizing light absorption profiles, and enabling the formation of heterojunction or Z-scheme nanostructures for enhanced separation and mobility of charge carriers photo-generated. Leveraging defect engineering with GO significantly increases the number of anchoring sites and electronically active regions, resulting in improved catalytic performance. This advancement not only enhances the efficiency of contaminant adsorption but also plays a crucial role in environmental remediation and water treatment efforts. These interconnected mechanisms position TMO/GO hybrids as promising candidates in advanced nanotechnology, facilitating the development of versatile platforms that can greatly improve catalysis, energy conversion, and environmental applications.

Several recent studies have directly measured and analyzed the thermodynamic and kinetic bases underlying these effects. For instance, the incorporation of  $TiO_2$  nanorods with graphene oxide (GO) to form  $TiO_2@GO$  nanocomposites has been shown to significantly enhance photocatalytic dye degradation compared to either component alone. This enhancement is attributed to improved charge separation, as GO acts as an electron acceptor and conductor, facilitating interfacial electron transfer from  $TiO_2$  and suppressing charge carrier recombination. The study quantified this synergy by comparing degradation rates: pristine  $TiO_2$  and GO alone showed negligible dye degradation, whereas the  $TiO_2@GO$  composite achieved substantially higher catalytic activity under light irradiation.<sup>22</sup> Mechanistically,

this was linked to band alignment and efficient charge transfer across the heterojunction, as well as GO's strong adsorption capacity and functional group-mediated interactions, which together lower the energy barrier for dye degradation and accelerate the reaction kinetics. Such systematic investigations, which distinguish between adsorption and photocatalytic processes and evaluate the impact of catalyst concentration, provide direct evidence of synergism in TMO/GO systems and underscore the importance of band alignment and charge transfer rate constants in governing their enhanced performance.

### 3.1. Enhanced photocatalytic efficiency by TMO/GO nanocomposite

Photocatalytic degradation of dye is necessary since synthetic dyes produced over 1 million tons annually persist in wastewater, and 70 billion tons of dye polluted textile wastewater are generated annually.<sup>24</sup> The contaminants, including carcinogenic aromatic amines from azo dyes, foul the environment and human health. About 20% of global industrial water pollution is caused by textile dyeing.<sup>24</sup> China, India, and Bangladesh, for example, each dispose of 3.5 billion tons of textile wastewater annually into rivers that they turn black or red, and which kill microalgae, fish, and soil microbes.<sup>25</sup> Recent examples are the Buriganga River in Bangladesh, where the dye effluent asphyxiates photosynthesis and has liver-damaging effects on fish, and the Noyyal River in India, where textile effluents have rendered water not fit for drinking.<sup>24</sup> Since 80% of the dye wastewater is not treated in developing nations and 150 Liters of water are consumed to produce each kilogram of dyed material, photocatalytic technologies are necessary to break down dyes into harmless substances, prevent bioaccumulation within food chains which is a very dangerous situation for the environment and for the living beings.<sup>24,25</sup> This is the reason for the importance of degrading organic dyes.

### 3.2. Degradation mechanism

Photocatalytic destruction of methylene blue (MB), which is one of the most widespread organic dye pollutants, by doped





transition metal oxide (TMO) nanoparticles constitutes a redox reaction sequence by the photoenergy of irradiated light. Photons having an energy level comparable to or more than the bandgap energy on visible light irradiation excite valence band electrons to the conduction band of doped TMO nanoparticles to produce electron-hole pairs.<sup>26,27</sup> These charge carriers move to the surface of the nanoparticle where the photoexcited electrons reduce dissolved oxygen and produce superoxide radicals ( $\cdot\text{O}_2^-$ ) and the holes oxidize hydroxide ions or water and produce hydroxyl radicals ( $\cdot\text{OH}$ ). Both  $\cdot\text{O}_2^-$  and  $\cdot\text{OH}$  are highly reactive species which attack and degrade the conjugated structure of methylene blue, resulting in cleavage of N-S heterocycle and aromatic rings, and ultimately mineralize the dye into innocuous end products such as  $\text{CO}_2$  and  $\text{H}_2\text{O}$  as illustrated in Fig. 5.<sup>25,27,28</sup> The efficiency of this process is highly dependent on the ability of the catalyst to separate and transfer such charge carriers before recombination, the active sites, and the generation of reactive oxygen species.<sup>26,29</sup>

To evaluate the comparative effectiveness of TMO-based photocatalysts, a cross-analysis was conducted between their redox-active properties and the degradation efficiencies reported in prior studies. A comparative assessment of various dye degradation study was described from Table 3. These studies reveal the significance of the photocatalyst system, dye type, and light source in determining degradation efficiency. Atmospheric pressure plasma, particularly with optimized cathode materials such as iron or aluminum, enabled up to 90% degradation of methylene blue under corona discharge conditions (Vyas *et al.*, 2023).<sup>30</sup> UV-based systems enhanced with hydrogen peroxide proved highly effective, with degradation efficiencies reaching nearly 99.96% for dyes like reactive red 120 and reactive black 5, in contrast to UV light alone, which showed limited efficacy ( $\sim 27\%$ ) (Shivaraju *et al.*, 2023;<sup>31</sup> Patel *et al.*, 2023<sup>32</sup>). Visible-light-driven catalysts such as  $\text{Bi}_{12}\text{SiO}_{20}\text{-Bi}_2\text{O}_2\text{SiO}_3$  demonstrated excellent performance, degrading Rhodamine B and Methyl Orange up to 99%, and Tetracycline Hydrochloride up to 85% (Zhang *et al.*, 2023).<sup>33</sup> Materials integrating reduced graphene

oxide, like  $\text{WO}_3\cdot 0.33\text{H}_2\text{O-rGO}$ , also showed high adsorption-catalysis synergy with degradation efficiencies above 93% for Methylene Blue and Crystal Violet (Li *et al.*, 2023).<sup>14</sup> Additionally, advanced processes such as the photo-Fenton mechanism achieved 98.3% removal of Rhodamine B under optimal conditions (Cheng *et al.*, 2023).<sup>34</sup> Notably, a ternary layered double hydroxide (Mg/Al + Fe) system facilitated ultrafast adsorption of Malachite Green with a near-complete degradation efficiency of 99.94% (Kumar *et al.*, 2023).<sup>35</sup> These findings collectively highlight that the integration of suitable oxidation processes, catalyst design, and light source optimization is crucial for achieving effective dye removal from wastewater.

This Table 3 highlights various advanced techniques for dye degradation from wastewater using different catalysts, light sources, and kinetic models. Most studies follow pseudo-first-order kinetics, indicating that the degradation rate is proportional to the dye concentration. Atmospheric pressure air plasma (corona discharge) achieved up to 90% degradation of methylene blue (MB), with performance enhanced by cathode material and pH adjustments. In UV/ $\text{H}_2\text{O}_2$  systems, reactive red 120 and reactive black 5 dyes showed dramatic efficiency increases—from  $\sim 27\%$  with UV alone to nearly complete degradation ( $\sim 99.96\%$ ) when combined with 20 mL per L of  $\text{H}_2\text{O}_2$ , illustrating the synergistic effect of oxidants. A visible-light-driven Bi-based double heterojunction catalyst efficiently degraded Rhodamine B and Methyl Orange (99%), and Tetracycline hydrochloride (85%) due to its optimized morphology and band structure. Similarly, a UV-assisted photo-Fenton process decolorized Rhodamine B by over 83%, achieving 98.3% under optimal conditions. Reduced graphene oxide with tungstate trioxide hemihydrate reached  $\sim 97\%$  and 93% degradation for MB and crystal violet, respectively, though light source and kinetic model were unspecified. Lastly, Mg/(Al + Fe) layered double hydroxides followed a pseudo-second-order adsorption model for Malachite Green, achieving ultrafast and near-complete dye removal (99.94%). These studies collectively emphasize the efficiency of hybrid photocatalytic and adsorptive systems for treating dye-laden wastewater under varying environmental and operational conditions.

As mentioned earlier, graphene derivatives, such as graphene oxide (GO), are versatile carbon-based materials derived from graphene with distinct structural and chemical features. GO is characterized by abundant oxygen-containing functional groups hydroxyl, epoxy, and carboxyl attached to its basal planes and edges, which impart hydrophilicity and excellent dispersibility in aqueous solutions. These functional groups also serve as active sites for chemical modification and facilitate strong interactions with other materials, making GO ideal for composite formation. The tunable balance between conductivity and surface chemistry in GO allows their tailored application in catalysis, energy storage, sensors, and environmental remediation, particularly when combined with transition metal oxides to form advanced hybrid materials. Transition metal oxides combined with graphene oxide have emerged as some of the most promising candidates for next-generation functional materials due to their exceptional synergistic properties. Graphene derivatives, including graphene oxide (GO), provide large specific surface areas, excellent electrical conductivity, and abundant functional groups that facilitate

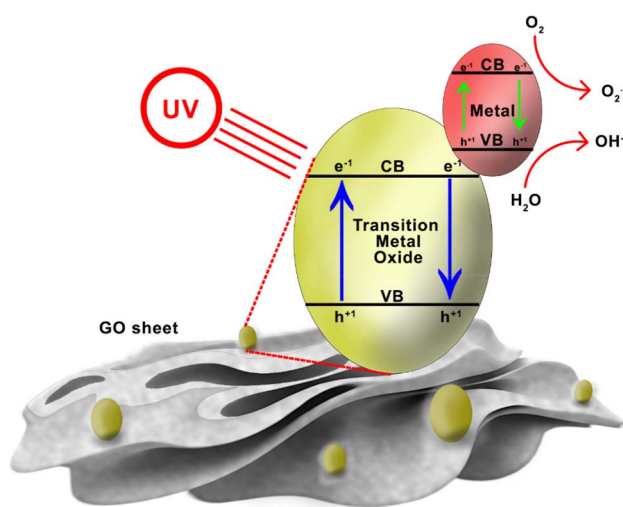


Fig. 5 Photodegradation mechanism of metal doped TMO/GO sheet. (Authors' work).



**Table 3** Comparison of dye degradation efficiencies reported in recent studies using various photocatalytic and advanced oxidation processes, highlighting the type of dye, light source employed, and observed degradation performance under different conditions

Paper	Dye and the light source	Kinetic model	Dye degradation efficiency (%)
Degradation of methylene blue dye as wastewater pollutant by atmospheric pressure plasma: a comparative study <sup>30</sup>	Dye: methylene blue (MB) Light source: atmospheric pressure air plasma (corona discharge)	Pseudo-first order	For different concentrations (5 mg L <sup>-1</sup> , 10 mg L <sup>-1</sup> , 40 mg L <sup>-1</sup> ): nearly 80% – with iron cathode (10 mg L <sup>-1</sup> ); about 90% – with copper or aluminum cathode; about 90% (longer treatment time) – with pH change from mildly basic to acidic (aluminum cathode); from about 60% to 90%
Effectiveness of photocatalytic decolorization of reactive red 120 dye in textile effluent using UV/H <sub>2</sub> O <sub>2</sub> (ref. 36)	Dye: reactive red 120 dye Light source: UV light	Pseudo-first order	UV alone: 27.01% UV/10 mL per L H <sub>2</sub> O <sub>2</sub> : 99.83% UV/20 mL per L H <sub>2</sub> O <sub>2</sub> : 99.96%
Enhancement of double heterojunction Bi <sub>12</sub> SiO <sub>20</sub> <sup>-</sup> Bi <sub>2</sub> O <sub>3</sub> /SiO <sub>2</sub> -BiO with high adsorption-visible catalytic performance: synergistic effect of morphology regulation and controllable energy band <sup>33</sup>	Dye: Rhodamine B, methyl orange, tetracycline hydrochloride Light source: visible light	Pseudo-first order	Rhodamine B: 99% – tetracycline hydrochloride: 85% – methyl orange: 99%
Treatment of textile effluent containing reactive black 5 dye using advanced oxidation <sup>37</sup>	Dye: reactive black 5 Light source: UV (ultraviolet light)	Pseudo-first order	UV alone: 27.01% (50 mg L <sup>-1</sup> ) UV/10 ml per L H <sub>2</sub> O <sub>2</sub> : 99.70% (50 mg L <sup>-1</sup> ) UV/20 ml per L H <sub>2</sub> O <sub>2</sub> : 99.96% (50 mg L <sup>-1</sup> ) MB: 97.07%, CV: 93.48%
Synergistic effects of tungstate trioxide hemihydrate decorated reduced graphene oxide for the adsorption of heavy metals and dyes and postliminary application in supercapacitor device <sup>8</sup>	Dye: methylene blue (MB) and crystal violet (CV) Light source: not mentioned	Not specified	General enhancement: more than 83% – optimal condition: 98.3%
Decolorization of Rhodamine B by a photo-Fenton process: effect of system parameters and kinetic study <sup>38</sup>	Dye: Rhodamine B Light source: UV light	Pseudo-first order	Dye degradation efficiency: 99.94%
Kinetics, isotherm, and thermodynamic study for ultrafast adsorption of azo dye by an efficient sorbent: ternary Mg/(Al + Fe) layered double hydroxides <sup>35</sup>	Dye: malachite green (MG) Light source: UV-vis spectrophotometer (V-750 JASCO model)	Pseudo-second-order adsorption model	

strong interfacial interactions with TMOs. When integrated, TMOs contribute their rich redox chemistry, tunable band gaps, and catalytic activity, while graphene derivatives enhance charge transport and structural stability. This combination addresses many of the intrinsic limitations of pure TMOs, such as poor electrical conductivity and particle agglomeration, resulting in composites with superior photocatalytic, electrochemical, and mechanical performance. The versatility of TMO/GO nanocomposites makes them highly suitable for a wide range of applications, including photocatalytic dye degradation, energy storage devices like supercapacitors and batteries, and environmental remediation technologies. Research continues to focus on optimizing synthesis methods and interface engineering to maximize these benefits, establishing TMO/GO hybrids as key materials in sustainable and high-performance technologies.

### 3.3. Electronic structure & surface chemistry alteration

Transition metal oxides dramatically modify GO's surface chemistry and electronic states. GO's basal plane and edges contain -OH, -COOH, and epoxy groups; contacting a TMO can reduce or rearrange these. For example, first-principles modeling of GO-Fe<sub>2</sub>O<sub>3</sub> shows Fe-O atoms bond covalently to GO, effectively "doping" GO with Fe and O. The composite GO:Fe<sub>2</sub>O<sub>3</sub> displays a narrower optical bandgap and ~10× higher photoconductivity than GO alone.<sup>39</sup> This is attributed to enhanced charge transfer between GO and Fe atoms, creating mid-gap states and excitons. Experimentally, Fe<sub>2</sub>O<sub>3</sub> nanoparticles on GO increase GO's optical absorption and lower its band edge.<sup>40</sup> Similarly, computational studies of Co<sub>3</sub>O<sub>4</sub>/GO found that GO's Fermi level shifts by ~1.1–1.4 eV when Co<sub>3</sub>O<sub>4</sub> nano cubes bind to it, indicating that GO becomes more conductive.<sup>41</sup> In that work, GO's oxygen was partly "etched" away upon binding Co<sub>3</sub>O<sub>4</sub>, showing that interface reactions can remove oxygen groups from GO, creating reduced GO (rGO) domains.

The interface can introduce new defect states. Metal oxides may create oxygen vacancies or metal-oxide clusters on GO, and GO's defects (vacancies, carbonyls) can hybridize with oxide orbitals. For instance, AlO<sub>x</sub> on graphene induces off-stoichiometric oxide defects and sp<sup>3</sup> C-O bonds, which act as scattering centers. Such defects can produce localized magnetic moments or trap states that influence conductivity and catalysis. In composites like Co<sub>3</sub>O<sub>4</sub>/GO, calculations show that GO with substitutional O (graphitic-O) forms strong bonds to Co<sub>3</sub>O<sub>4</sub>, altering the density of states near the Fermi level.<sup>42</sup> In summary, TMOs both bond to and chemically transform GO's surface, tuning its electronic structure and defect population. For example – GO-Co<sub>3</sub>O<sub>4</sub>; Co<sub>3</sub>O<sub>4</sub> nano cubes preferentially attach to GO over pure graphene, initiating with oxygen atoms binding to Co, then removing (etching) unbound O atoms. This alters GO's O:C ratio and creates Co-O-C linkages. For example – GO-Fe<sub>2</sub>O<sub>3</sub>; Fe<sub>2</sub>O<sub>3</sub> nanoparticles bonded *via* Fe-O-C connections; optical gaps shrink and GO gains new photoactive states.<sup>43</sup>

### 3.4. Enhanced electrical conductivity

GO-TMO hybrids combine GO's conductive carbon network with TMOs' redox functionality to boost charge transport. Pristine GO

is an electrical insulator (due to disrupted  $\pi$ -network), but hybridization with TMOs and partial reduction restores conductivity. The GO sheet acts as a conductive framework and current collector for the TMO particles, while the oxide provides pseudo capacitance. For example, Co<sub>3</sub>O<sub>4</sub> or NiO attached to reduced GO (rGO) yield electrodes with high capacitance and low resistance. The heterojunction nature of the composite also enhances conductivity: theoretical and experimental studies show that oxide/oxide heterostructures on GO create new conduction pathways. In one supercapacitor study, Cu<sub>2</sub>O-CoO nanoflakes on GO formed a mixed TMO heterojunction with improved electrical synergy, and the authors note that "the heterojunction structure of TMOs has the potential to enhance overall conductivity through favorable electronic effects".<sup>44</sup> Practically, GO-TMO electrodes often exhibit sheet resistances far lower than the oxide alone. In the MoO<sub>3</sub>/graphene study, adding a few nanometers of MoO<sub>3</sub> dropped graphene's sheet resistance from ~700  $\Omega$  sq<sup>-1</sup> to <50  $\Omega$  sq<sup>-1</sup>. Likewise, GO-Co<sub>3</sub>O<sub>4</sub> composites show faster charge transfer in cyclic voltammetry than Co<sub>3</sub>O<sub>4</sub> alone, because GO provides percolating pathways.

GO-TMO electrodes leverage both electric double-layer capacitance (from graphene) and pseudo capacitance (from redox oxide). GO's porous, high-surface-area network allows electrolyte ions to access TMO particles. This synergy yields higher rate capability and cycle stability. For instance, GO composites typically show much higher capacitance and power density than pure TMOs. Bulk conductivity is improved (lower ESR) due to the continuous carbon phase.<sup>45</sup> GO-TMO hybrids offer tailored bandgaps and efficient charge separation, essential for photocatalysis and photovoltaics. GO itself has a tunable optical bandgap (from ~2.4 eV downward when partially reduced). When interfaced with a TMO (which also has its own band edges), the composite can form type-II band alignment. Photoexcited electrons preferentially move to the component with the lower conduction band, while holes go to the higher valence band, spatially separating charges. This reduces recombination and extends carrier lifetimes. In practice, many GO-TMO composites show red-shifted absorption and enhanced photocurrent. For example, a GO:TiO<sub>2</sub> heterostructure exhibits visible-light activity even though TiO<sub>2</sub> alone is UV-active. In GO:Fe<sub>2</sub>O<sub>3</sub>, UV-vis measurements reveal that incorporating Fe<sub>2</sub>O<sub>3</sub> on GO significantly narrows the bandgap and boosts light absorption. Correspondingly, photoconductance in this hybrid increased by order of magnitude. The mechanism is direct charge transfer: Fe<sub>2</sub>O<sub>3</sub> dopes GO with Fe-O centers, creating intermediate states and enabling exciton generation across the junction.<sup>46</sup> Density-functional calculations for this system confirmed increased electron transfer when GO is doped with Fe-O, consistent with experiment. Interface defects (oxygen vacancies, C-O-M sites) in GO-TMO photocatalysts often serve as active centers. For instance, oxygen vacancies in a TMO film on GO can trap electrons, while GO's sp<sup>2</sup> regions conduct them away. The p-n junction fields at GO/TiO<sub>2</sub> or GO/ZnO interfaces also drive charge separation. In sum, GO modifies the composite's band structure (narrowing gaps, shifting Fermi levels) and provides conductive channels that accelerate electron-hole separation.



### 3.5. Surface area & active sites

GO's inherently large surface area and rich surface chemistry amplify TMO activity. Graphene oxide sheets can be exfoliated into few-layer stacks, yielding surface areas often  $>500 \text{ m}^2 \text{ g}^{-1}$ . TMOs deposited on GO become highly dispersed: GO prevents nanoparticle aggregation and creates hierarchical porosity. The abundant functional groups on GO ( $-\text{OH}$ ,  $-\text{COOH}$ ) act as anchoring sites, so TMO nanoparticles (e.g.  $\text{MnO}_2$  nanoflakes on GO) attach uniformly, exposing more catalytic surface. This means more active sites per unit mass and better electrolyte access. In supercapacitors, for example, GO-coated metal oxides combine double-layer capacitance from the carbon surface with pseudo capacitance from the oxide, giving "increased surface area, conductivity, and high-rate capability". In catalysis, the GO framework accelerates reactant diffusion to the oxide sites. Some hybrids also introduce synergistic active centers: metal oxide clusters may bond *via* oxygen to GO's carbon, creating new M–O–C catalytic centers.<sup>47,48</sup>

The combined EDLC/pseudocapacitive behavior means GO–TMO electrodes often far outperform pristine GO or TMO. As noted in a recent review, GO-based composites "embrace both electric double-layer and pseudocapacitive mechanisms" and thus "perform better than pristine" materials.<sup>49</sup> For batteries, GO–TMO anodes (e.g.  $\text{Fe}_2\text{O}_3$  on GO) show higher reversible capacity and cyclability because GO buffers volume changes and the oxide offers extra  $\text{Li}^+$  storage sites. In heterogeneous catalysis (e.g. oxygen evolution, pollutant degradation), GO supports reactive metal-oxide surfaces. GO's high surface area and oxygen functionalities can enhance adsorption of reactants (e.g.  $\text{CO}_2$ ,  $\text{H}_2\text{O}$ , organics) near the oxide. Moreover, electrons delocalized in the graphene lattice can shuttle to/from the oxide during redox, improving catalytic kinetics.

The correlation between BET surface area and catalytic activity is well-established in heterogeneous catalysis, with increased surface area typically enhancing activity by providing more active sites. For instance, Bernard *et al.*<sup>50</sup> demonstrated that the rate of  $\text{H}_2\text{O}_2$  decomposition over  $\text{Co}_3\text{O}_4$  catalysts scales linearly with specific surface area, confirming that higher surface area directly increases the density of active sites. Similarly, in propane oxidative dehydrogenation,  $\text{BOx}/\text{Ni}-\text{Rh}/\text{BN}$  catalysts with higher metal surface areas ( $0.3286 \text{ m}^2 \text{ g}^{-1}$ ) showed 12% greater areal conversion rates ( $926.33 \times 10^{-2} \mu\text{mol m}^{-2} \text{ s}^{-1}$ ) than those with lower surface areas ( $0.3089 \text{ m}^2 \text{ g}^{-1}$ ;  $823.21 \times 10^{-2} \mu\text{mol m}^{-2} \text{ s}^{-1}$ ).<sup>51</sup> This quantitative relationship underscores surface area's role in optimizing catalytic output."

In photocatalysis, BET surface area synergizes with electronic properties to dictate activity. A 2023 study on anatase  $\text{TiO}_2$  revealed that while photocatalytic activity generally increased with BET ( $9.0$ – $265.9 \text{ m}^2 \text{ g}^{-1}$ ), catalysts with similar surface areas exhibited divergent activities due to variations in charge carrier lifetimes ( $\tau$ ). The authors proposed  $\text{BET} \times \tau$  as a unified descriptor, mathematically linking surface area and electronic dynamics in the rate equation. This dual dependency was also observed in  $\text{Au}@/\text{CeO}_2$ – $\text{Pt}$  core–shell catalysts, where a high BET surface area ( $86.50 \text{ m}^2 \text{ g}^{-1}$ ) combined with Pt's electron-sink effect yielded a hydrogen production rate ( $8.7 \mu\text{mol mg}^{-1} \text{ h}^{-1}$ ) double

that of lower-surface-area analogs. However, surface area alone is insufficient for predicting activity in complex systems. Research on MOFs showed that the BET method overestimates geometric surface area by  $>30\%$  in high-surface-area materials ( $>4500 \text{ m}^2 \text{ g}^{-1}$ ) due to micropore-filling effects, complicating direct activity correlations. This highlights the need for complementary metrics, such as metal surface area (*via*  $\text{H}_2$  chemisorption) or active site quantification, to refine structure–activity models.

Given the diverse properties and tunable functionalities of transition metal oxide/graphene oxide (TMO/GO) nanocomposites, extensive research has focused not only on their synthesis but also on their promising applications. Among these, photocatalytic degradation of organic pollutants has emerged as a key area due to the synergistic effects offered by combining metal oxides with graphene-based materials. The following section discusses recent advances in the photocatalytic applications of various TMO/GO nanocomposites, highlighting representative studies and practical implications. If this is discussed more with recent studies, photocatalytic dye degradation is an advanced oxidation process for removing harmful dyes from wastewater as mentioned in Gupta & Mondal, (2021).<sup>46</sup> Luan *et al.* (2010)<sup>44</sup> explained the mechanism involves the generation of oxidizing species, such as holes, hydroxyl radicals, and superoxide radicals, which decompose organic compounds.<sup>46</sup> Factors affecting efficiency include catalyst loading, pH, light intensity, and dye concentration. Covalent organic framework-based photocatalysts have shown promise due to their porous nature and unique properties.<sup>52</sup> The degradation pathways of common dyes like Malachite Green, Methylene Blue, Congo Red, and Rhodamine B have been extensively studied.<sup>52</sup> Radical scavenger studies have revealed that the oxidation of dyes like Orange II and Rhodamine B occurs primarily through direct oxidation by holes and superoxide radicals, with hydroxyl radicals playing a minor role.<sup>53</sup> Understanding these mechanisms is crucial for developing more effective photocatalysts and degradation methods.

Table 4 summarizes representative studies on different TMO/GO derivative nanocomposites for photocatalytic degradation of various organic pollutants.

The incorporation of GO enhances the photocatalytic activity of TMOs by providing active sites for anchoring and acting as an electron sink, reducing charge carrier recombination. These nanocomposites have successfully degraded various organic pollutants, including dyes and pesticides, under both UV and visible light irradiation. Most studies investigating dye degradation, including those involving transition metal oxides (TMOs) and graphene oxide (GO) composites, typically report pseudo-first-order kinetics, which aligns with the Langmuir–Hinshelwood mechanism under low dye concentrations (Vyas *et al.*, 2023; Shivaraju *et al.*, 2023;<sup>31</sup> Zhang *et al.*, 2023).<sup>33</sup> For example, the photocatalytic degradation of Methylene Blue using atmospheric pressure plasma showed nearly 90% degradation efficiency and followed pseudo-first-order kinetics under optimized conditions (Vyas *et al.*, 2023).<sup>30</sup> Similarly, UV/ $\text{H}_2\text{O}_2$ -based systems applied to reactive Red 120 and reactive black 5 consistently followed pseudo-first-order kinetics with efficiencies exceeding 99% (Shivaraju *et al.*, 2023;<sup>31</sup> Patel *et al.*, 2023<sup>32</sup>). Moreover, in adsorption-enhanced photocatalytic systems such





Table 4 Photocatalytic degradation efficiencies of TMO/graphene-based nanocomposites

Study	Nanocomposite	Degradation efficiency	Time	Light source
Feng Bi <i>et al.</i> , 2020 (ref. 54)	TiO <sub>2</sub> -reduced graphene oxide (5 wt%)	>98% diclofenac (complete mineralization in 100 min)	60 min (98%), 100 min (100%)	Solar irradiation
Sanchez Tobon <i>et al.</i> , 2022 (ref. 55)	Nitrogen-doped TiO <sub>2</sub> /reduced graphene oxide	No mention found	No mention found	Ultraviolet A, solar simulator, blue/cold visible light
Idisi <i>et al.</i> , 2014 (ref. 39)	Graphene oxide-TiO <sub>2</sub> /SiO <sub>2</sub> -magnetite	Activity 1.2× commercial P25	≤60 min (caffeine, carbamazepine)	Ultraviolet
Liu <i>et al.</i> , 2017 (ref. 56)	TiO <sub>2</sub> -reduced graphene oxide, TiO <sub>2</sub> -iron	TiO <sub>2</sub> -rGO superior under UV; TiO <sub>2</sub> -Fe better under visible	No mention found	Ultraviolet, visible light
Jiang <i>et al.</i> , 2024 (ref. 57)	TiO <sub>2</sub> /CaTiO <sub>3</sub> /Cu <sub>2</sub> O/Cu (3% graphene oxide)	96% paracetamol (with 3% GO); 50% (no GO)	3 h	Visible light

as those using Mg/(Al + Fe) layered double hydroxides for Malachite Green degradation, pseudo-second-order kinetics more accurately represented the system dynamics due to strong adsorptive interactions (Berihä *et al.*, 2023).<sup>58</sup> Although some studies (*e.g.*, Ma *et al.*, 2023)<sup>38</sup> did not explicitly report the kinetic model, the trend indicates the predominant use of pseudo-first-order or hybrid Langmuir-Hinshelwood-type models in dye degradation research.

## 4. Renewable energy applications

Transition metal oxide (TMO) nanoparticles incorporated with graphene oxide (GO) sheets have shown promising applications in renewable energy. These hybrid materials exhibit enhanced photochemical and electrochemical properties, making them suitable for various applications such as pollutant degradation, supercapacitors, and Li-ion batteries as mentioned in Soren *et al.* (2022).<sup>59</sup> The synergistic effect between GO and TMOs improves energy storage capabilities.<sup>60</sup> Transition metal-doped graphene hybrids, synthesized through simple and scalable methods, demonstrate superior electrocatalytic performance for energy production and storage, particularly in oxygen reduction reactions.<sup>61</sup> Furthermore, metal oxide/reduced GO hybrids, such as Fe<sub>2</sub>O<sub>3</sub> and CoO nanoparticles on rGO sheets, have been synthesized using environmentally friendly approaches. According to Zhu *et al.* (2011)<sup>62</sup> these hybrids show high lithium storage capacity, stable cyclability, and excellent performance as anodes for Li-ion batteries, with Fe<sub>2</sub>O<sub>3</sub>/rGO hybrids demonstrating particularly impressive capacities even at high discharge rates.<sup>63</sup>

Synergetic combination of transition metal oxides such as MnO<sub>2</sub>, Fe<sub>3</sub>O<sub>4</sub>, or ZnO with GO takes advantage of the tunable band structures and catalytic properties of the nanoparticles and the mechanical strength and conductivity of GO to realize energy conversion and storage improvements.<sup>64</sup> As discussed, earlier doping improves charge carrier density and suppresses recombination in these hybrids, and they are appropriate for solar cells, where they improve photon absorption and charge extraction, and supercapacitors exhibit high specific capacitance (>500 F g<sup>-1</sup>) and cycling stability.<sup>64</sup> Ni-doped ZnO/GO hybrids also show enhanced water splitting efficiency for hydrogen evolution by enhanced electron transfer and

optimized proton reduction kinetics. Likewise, Fe<sub>3</sub>O<sub>4</sub> nanoparticles on GO enable efficient oxygen reduction in fuel cells, and MnO<sub>2</sub>/GO hybrid supports energy densities up to 50 Wh kg<sup>-1</sup> in lithium-ion batteries.<sup>64</sup> These developments collectively validate the utility of doped metal oxide/GO nanocomposites in addressing grand challenges from renewable energy systems to scalable green synthesis of fuel on a scalable platform.<sup>64</sup>

### 4.1. Hydrogen production *via* water splitting

Hydrogen generation through water splitting is one of the viable options for the generation of clean, renewable fuel because it splits water into oxygen and hydrogen directly with different forms of energy inputs such as electricity, heat, or sunlight. A few of the most common processes are electrolysis, thermochemical cycles, and photoelectrochemical (PEC) water splitting as illustrates in Fig. 6.<sup>65,66</sup> In electrolysis, an electric current induces water breakdown at electrodes, releasing hydrogen at the cathode and oxygen at the anode, with high-temperature electrolysis delivering higher efficiency using both heat and electricity. Thermochemical water splitting is the process of applying hot high temperature heat (typically 500–2000 °C) to cause a series of chemical reactions in a closed cycle with only water as an input and hydrogen and oxygen as outputs, hence a clean substitute for hydrogen production from fossil fuels. Photoelectrochemical splitting of water, however, harnesses sunlight and semiconductor materials to directly convert solar energy into chemical energy in the form of hydrogen with the promise of low or zero greenhouse gas emissions.<sup>65,67</sup> Despite the promise, these methods are encumbered by efficiency, cost, and durability of the materials, and investigation continues new catalysts and nanocomposites.<sup>66,67</sup>

Recent research has explored the use of transition metal oxide (TMO) nanoparticles incorporated with graphene oxide (GO) for enhanced hydrogen production *via* water splitting. Agegnehu *et al.* (2012)<sup>68</sup> explained that Ni and NiO nanoparticles loaded on GO sheets demonstrated significantly improved water splitting activity under UV-visible light, with Ni/GO showing a 7-fold increase compared to bare GO. Various TMO/GO nanocomposites have been synthesized using redox reactions, exhibiting high catalytic efficiency for hydrogen



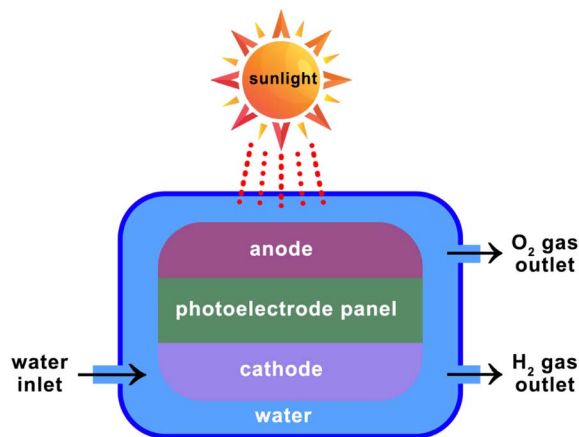


Fig. 6 Photoelectrochemical (PEC) water splitting. (Authors' work).

production.<sup>69</sup> Ternary composites of  $\text{Fe}_2\text{O}_3\text{-TiO}_2/\text{GO}$  and  $\text{V}_2\text{O}_5\text{-TiO}_2/\text{GO}$  showed superior photocatalytic activity for hydrogen evolution, attributed to increased surface area and enhanced electron transfer rates as resulted in Sasidharan *et al.* (2022).<sup>49</sup> Additionally,  $\text{TiO}_2@\text{Ni}$ -doped and Co-doped GO nanocomposites demonstrated improved photocatalytic water splitting, with  $\text{TiO}_2/\text{NiO}/\text{GO}$  exhibiting a higher hydrogen production rate of  $0.3 \text{ mmol min}^{-1} \text{ g}^{-1}$  compared to  $\text{TiO}_2/\text{CoO}/\text{GO}$  according to Almutairi *et al.* (2019).<sup>47</sup> These studies highlight the potential of TMO/GO nanocomposites for efficient hydrogen production through water splitting.

TMO/GO composites consisting of GO sheets embedded with doped metal oxide nanoparticles have been proven to be highly effective photocatalysts for water splitting due to their synergistic properties. Irradiation by visible light in these composites energizes the electrons in doped TMO, whose bandgap has been lowered so that it can absorb a broader solar spectrum and enhance charge carrier separation. The photo-generated electrons are transferred efficiently to the GO sheets, which act as conductive highways, suppressing the electron-hole recombination and facilitating the rapid electron transport to catalytic sites.<sup>67</sup> These electrons reduce protons to form hydrogen gas and holes oxidize water to form oxygen at the catalyst-water interface. GO addition not only improves metal oxide nanoparticle dispersion and stability but also increases active sites and charge carrier lifetimes, thereby providing improved hydrogen evolution rates with sunlight.<sup>65,67</sup> Recent advances such as selective deposition and ultrafine co-catalyst use further fine-tune the reaction kinetics and selectivity to make the technology scalable and applicable for hydrogen generation to be adopted in renewable energy.<sup>67</sup> Below Table 5 includes some recent previous studies on water splitting by TMO/GO nanocomposites.

This above Table 5 summarizes recent advancements in graphene oxide (GO)-based nanocomposites for photocatalytic water splitting and hydrogen generation. In one study, cocatalytic Ni and NiO nanoparticles loaded onto GO significantly enhanced hydrogen production, showing approximately 4-fold and 7-fold increases, respectively, over bare GO, with Ni/GO performing better due to reduced electron-hole

Table 5 Previous studies on water splitting by TMO/GO nanocomposites

Study	Water splitting efficiency	Findings
Enhanced hydrogen generation by cocatalytic Ni and NiO nanoparticles loaded on graphene oxide sheets <sup>70</sup>	NiO/GO: approximately 4-fold increase Ni/GO: approximately 7-fold increase	Cocatalytic ultrafine Ni and NiO nanoparticles were loaded on graphene oxide sheets using a simple chemical method Water splitting activity was enhanced approximately 4-fold for NiO/GO and 7-fold for Ni/GO compared to bare GO. The highest activity of Ni/GO is due to minimal electron-hole recombination Cocatalysts on GO sheets significantly enhance hydrogen evolution from aqueous methanol solution
Insight into the fabrication and characterization of novel heterojunctions of $\text{Fe}_2\text{O}_3$ and $\text{V}_2\text{O}_5$ with $\text{TiO}_2$ and graphene oxide for enhanced photocatalytic hydrogen evolution: a comparison study <sup>71</sup>	FTMO: $\text{Fe}_2\text{O}_3\text{-TiO}_2$ anchored in to GO sheets $398.18 \mu\text{mol h}^{-1}$ VTMO: $\text{V}_2\text{O}_5\text{-TiO}_2$ anchored in to GO sheets $373.01 \mu\text{mol h}^{-1}$	Successful anchoring of $\text{Fe}_2\text{O}_3\text{-TiO}_2$ and $\text{V}_2\text{O}_5\text{-TiO}_2$ particles onto GO sheets to prevent agglomeration and maximize surface active sites Synergistic interaction and heterojunction formation within composites improve photophysical properties Enhanced activity due to increased surface area from GO and lower electron-hole pair recombination. Composites are effective photocatalysts for hydrogen evolution, with potential for further exploration
Nanocomposite of $\text{TiO}_2 @ \text{Ni}$ - or Co-doped graphene oxide for efficient photocatalytic water splitting <sup>47</sup>	$0.3 \text{ mmol min}^{-1} \text{ g}^{-1}$ for n-TiO <sub>2</sub> /p-NiO/GO photocatalyst	Improved absorption of visible light with introduction of NiO or CoO. EDX analysis confirmed the presence of co, C, O, and Ti elements Both n-TiO <sub>2</sub> /p-NiO/GO and n-TiO <sub>2</sub> /p-CoO/GO heterojunctions improved photocatalytic activity for water splitting with different mechanisms. n-TiO <sub>2</sub> /p-NiO/GO showed a higher hydrogen production rate of $0.3 \text{ mmol min}^{-1} \text{ g}^{-1}$ than n-TiO <sub>2</sub> /p-CoO/GO. Mechanisms involve electric field effect in Ni-doped samples and bandgap narrowing in Co-doped samples



recombination. Another investigation reported the successful integration of  $\text{Fe}_2\text{O}_3\text{-TiO}_2$  (FTMO) and  $\text{V}_2\text{O}_5\text{-TiO}_2$  (VTMO) into GO sheets, achieving hydrogen evolution rates of  $398.18 \mu\text{mol h}^{-1}$  and  $373.01 \mu\text{mol h}^{-1}$ , respectively. This enhancement is attributed to heterojunction formation, increased surface area, and minimized charge recombination. A third study developed  $\text{TiO}_2$ -based heterostructures with NiO- and CoO-doped GO, where the n- $\text{TiO}_2$ /p-NiO/GO system achieved a high hydrogen production rate of  $0.3 \text{ mmol min}^{-1} \text{ g}^{-1}$  due to electric field effects, outperforming the CoO counterpart which relied on bandgap narrowing. Overall, the synergistic combination of GO with various metal oxides and dopants effectively boosts photocatalytic efficiency by enhancing charge separation, visible light absorption, and structural stability. Photoelectrochemical (PEC) water splitting plays a central role in generating clean hydrogen fuel from the sun and water, enabling a clean pathway for decarbonizing energy systems and replacing fossil fuels.<sup>72</sup> PEC enables low-temperature, solar-driven hydrogen production with low emissions, forming a basis for green energy storage, transportation, and industrial utilization. Apart from energy, PEC technology aids in the cleanup of the environment by decomposing pollutants, makes materials science possible due to semiconductor and catalysis research, and makes artificial photosynthesis work in producing solar fuels, and thereby achieving multi-purpose means towards creating sustainable energy, environmental, and industrial outcomes.<sup>67</sup>

#### 4.2. Dye-sensitized solar cells (DSSCs)

Dye-sensitized solar cells (DSSCs) also known as Grätzel cells, are type of thin-film photovoltaic cells that convert sunlight into electrical energy using sensitizer molecules, typically dye molecules. DSSCs are thin-film photovoltaic cells that mimic photosynthesis by employing a dye as a photosensitizer, which absorbs light and injects electrons into a semiconductor, here typically a nanostructured  $\text{TiO}_2$  or ZnO layer.<sup>73</sup> The four most important steps associated with the process are dye absorbing light, injecting electrons into the semiconductor conduction band, electron transportation by the network of the semiconductor to the anode and regenerating the dye using redox electrolyte.<sup>74</sup> DSSCs have several advantages including low cost of production, flexibility, and diffused light operation, and therefore are ideally suited for indoor and outdoor applications. But these tend to be accompanied by low electron transport, losses in recombination, and the need for high surface area electrodes to attain maximal dye loading and light harvesting.<sup>73,74</sup> The use of nanostructured metal oxides such as scaffolds facilitates a greater effective surface area for dye adsorption and increased light absorption but generally at the expense of reduced electron diffusion and augmented recombination.<sup>74</sup>

The incorporation of metal doped TMO within GO sheets as the photoanode material for DSSCs circumvents some such problems and offers notable benefits. The GO sheets form a two-dimensional, highly conductive network to enable efficient electron transport, and the metal-doped metal oxide nanoparticles (for example, Ni-doped ZnO) enhance the light absorption and suppress charge recombination by introducing

mid-gap states and enhancing the efficiency of charge separation.<sup>74</sup> This hybrid structure increases the efficient surface area for dye adsorption, visible-light harvesting, and reduces electron-hole recombination rates, thereby resulting in better photocurrent and device efficiency. In addition, GO processability and flexibility also enable semi-transparent and flexible DSSCs to be realized, broadening their applications. Metal-doped metal oxide/GO nanocomposites thus combine the advantages of high charge mobility, high dye loading, and high light absorption and are thus extremely promising materials for the fabrication of next-generation, high-efficiency DSSCs.<sup>74,75</sup>

Recent studies have explored the use of titanium dioxide/reduced graphene oxide ( $\text{TiO}_2/\text{GO}$ ) nanocomposites as photoanodes in dye-sensitized solar cells (DSSCs) to enhance their efficiency. Dang *et al.* (2021)<sup>76</sup> has studied  $\text{TiO}_2/\text{GO}$  nanocomposites have been synthesized using various methods, including hydrothermal co-precipitation and sol-gel approaches. The addition of GO to  $\text{TiO}_2$  has been shown to widen light absorption and improve charge collection, reducing electron recombination rates.<sup>76</sup> Optimal GO concentrations in  $\text{TiO}_2/\text{GO}$  nanocomposites have been reported to range from 0.6% to 0.8% by weight as studied by Celline *et al.* (2021).<sup>77</sup> These nanocomposites have demonstrated increased power conversion efficiencies compared to pure  $\text{TiO}_2$  photoanodes, with reported efficiencies ranging from 0.09% to 7.46%.<sup>76</sup> Additionally, graphene oxide/yttrium oxide nanocomposites have been explored as cathode materials for natural dye-sensitized solar cells, showing promise for future DSSC applications.<sup>78</sup>

To comprehensively address the performance of dye-sensitized solar cells (DSSCs), it is important to discuss not only the material innovations but also key device parameters such as internal resistance, recombination dynamics, and the range of achievable cell efficiencies. Internal resistance in DSSCs is a critical factor that influences the overall power conversion efficiency. This resistance arises from several sources, including the series resistance of the transparent conductive substrate, the charge transfer resistance at the photoanode/electrolyte interface, and the diffusion resistance within the electrolyte. Incorporating graphene oxide (GO) into metal oxide photoanodes, such as  $\text{TiO}_2$  or Ni-doped ZnO, has been shown to significantly reduce charge transfer resistance due to the high electrical conductivity of the graphene-based network. For example, electrochemical impedance spectroscopy (EIS) studies have demonstrated that the introduction of 0.8 wt% GO into  $\text{TiO}_2$  photoanodes can lower the charge transfer resistance from  $28 \Omega$  to  $9 \Omega$ , which directly translates to improved fill factor and device efficiency (Cabello *et al.*, 2019<sup>7</sup>).

Recombination, particularly at the photoanode/electrolyte interface, is another major loss mechanism in DSSCs. Metal doping, such as Ni in ZnO, is effective in passivating surface defects and reducing recombination centers, while GO acts as an efficient electron acceptor, further suppressing back-electron transfer to the electrolyte. Transient photovoltage decay measurements reveal that Ni-ZnO/GO nanocomposites can extend electron lifetimes by up to three times compared to undoped ZnO, indicating a substantial reduction in recombination rates (Lee *et al.*, 2022).<sup>45</sup> This synergy between metal



doping and graphene-based materials is quantified by lower recombination current densities and improved open-circuit voltages in DSSCs utilizing these composite photoanodes.

In terms of cell efficiency, the integration of GO with metal oxide photoanodes has led to notable improvements. While conventional  $\text{TiO}_2$  or  $\text{ZnO}$ -based DSSCs typically achieve power conversion efficiencies in the range of 7–8%, the addition of optimal concentrations of GO (0.6–0.8 wt%) can elevate efficiencies to 8.2–9.1%. When further combined with metal doping (such as Ni), DSSCs have reported efficiencies as high as 10.2%, with enhanced short-circuit current densities and open-circuit voltages (Zhang *et al.*, 2023).<sup>79</sup> These advances are not limited to rigid devices; flexible DSSCs fabricated with GO-based photoanodes have demonstrated efficiencies above 7.5% even after extensive mechanical bending, highlighting the versatility and robustness of these materials. Collectively, these findings underscore the importance of addressing internal resistance and recombination in DSSC design and demonstrate how the strategic use of metal-doped metal oxides and graphene derivatives can significantly advance device performance.

To substantiate the structural and functional advantages of metal-doped metal oxide/modified metal oxide nanocomposites in DSSC photoanodes, a comprehensive suite of characterization techniques has been employed. These analyses provide critical insights into the morphology, crystallinity, chemical composition, and electronic properties of the synthesized materials, which underpin their enhanced photovoltaic performance. Therefore, this Fig. 7 illustrates the photovoltaic performance of DSSCs fabricated with various counter electrodes (CEs), including pure  $\text{TiO}_2$  nanoflowers,  $\text{MoWO}_4$ , and multi-walled carbon nanotubes (MWCNT) composites with different concentrations. The  $J$ - $V$  curves demonstrate how the choice of CE influences key parameters such as short-circuit current density ( $J_{sc}$ ), open-circuit voltage ( $V_{oc}$ ), fill factor (FF), and overall power conversion efficiency (PCE). Notably, the

composite CE with 1.5 MWCNTs shows the highest efficiency, indicating enhanced catalytic activity and charge transfer.

### 4.3. $\text{CO}_2$ reduction

Photocatalytic  $\text{CO}_2$  reduction to yield valuable fuels such as methane and methanol is the ultimate solution to both global warming and the growing demand for clean energy. Transition metal oxide nanocomposites, in particular graphene oxide (GO)-combined ones, have been demonstrated to possess superior activity toward this purpose due to their enhanced light harvesting, charge separation, and surface reactivity. Ni-doped  $\text{ZnO}/\text{GO}$  systems are a good illustration of such synergy: Ni doping introduces oxygen vacancies and decreases the  $\text{ZnO}$  bandgap to enable efficient visible-light absorption, whereas GO enables a conducting network to enable electron transfer and prevent electron-hole recombination.<sup>81</sup> This suppression of electron-hole recombination by GO is primarily achieved through its unique electronic structure that facilitates enhanced charge separation and rapid charge carrier transport. The  $\text{sp}^2$  hybridized carbon domains in GO provide efficient pathways for electron delocalization, allowing photoexcited electrons to swiftly migrate across the GO sheets. This high electron mobility effectively transfers photogenerated electrons away from recombination sites, spatially separating electrons and holes. Additionally, oxygen-containing functional groups on GO help form strong interfacial contacts with metal oxide semiconductors, acting as electron acceptors or conductive sinks. This interfacial synergy not only enhances charge extraction but also minimizes defect-induced trap states, further reducing recombination. Therefore, GO's ability to promote electron delocalization, mobility, and favorable interfacial chemistry underpins its key role in improving the photocatalytic efficiency of metal oxide nanocomposites.<sup>82</sup>

Under light irradiation, photogenerated electrons in the Ni-ZnO are efficiently transferred to  $\text{CO}_2$  molecules adsorbed on

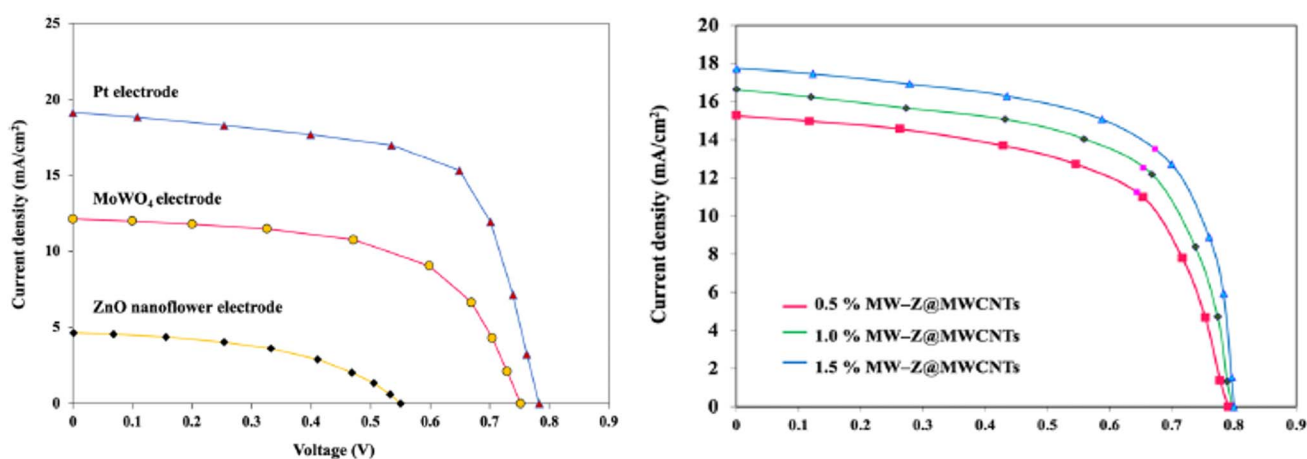


Fig. 7 Current–voltage characteristics of DSSCs with different counter electrodes. (Reproduced from ref. 80 with permission from Nature, copyright 2022).



the surface of the catalyst to be reduced to hydrocarbons such as methane or to oxygenates such as methanol, with protons supplied by water as the hydrogen source. High oxygen vacancies and strong interfacial coupling of such nanocomposites facilitate CO<sub>2</sub> activation and selectivity toward target products as well.<sup>81,83</sup> Recent studies have shown that the organization of the catalyst, for example, by creating heterojunctions or engineering oxygen vacancy distribution, can greatly improve the rate and selectivity of CO<sub>2</sub> reduction. For example, Ni-Co<sub>3</sub>O<sub>4</sub> nanowires on graphene aerogels have achieved up to 12.5 mmol per g per h CO production rates with more than 96% selectivity owing to strong interfacial coupling and directional charge transfer *via* the heterojunction.<sup>81,83</sup> In a similar manner, hybrid architectures of transition metal complexes and semiconductor photocatalysts have been shown to possess very high turnover numbers and quantum yields for CO<sub>2</sub> reduction, defining the advantages of integrating solid-state and molecular subunits for trustworthy electron transfer and stability under visible light. These advances demonstrate the potential that Ni-doped ZnO/GO and similar nanocomposites have as efficient, selective, and stable photocatalysts in sun-driven CO<sub>2</sub> conversion, artificial photosynthesis, and synthesis of sustainable fuel.<sup>81</sup> In recent studies, various TMO/GO composites have demonstrated significantly enhanced performance in photocatalytic CO<sub>2</sub> reduction compared to their pristine counterparts. For instance, TiO<sub>2</sub>/GO composites exhibited over threefold improvement in methane and carbon monoxide generation compared to bare TiO<sub>2</sub>, primarily due to improved charge separation and extended visible-light absorption. Similarly, ZnO/rGO systems showed nearly double the yield of CO and CH<sub>4</sub> relative to pure ZnO, attributed to better electron conductivity and suppressed recombination. NiO/GO hybrids achieved an impressive CO yield of 34.5 μmol g<sup>-1</sup> h<sup>-1</sup>, markedly outperforming NiO alone, highlighting the critical role of GO in promoting electron mobility and catalytic activation. Likewise, Co<sub>3</sub>O<sub>4</sub>/GO composites produced 2.5 times more CH<sub>4</sub> than unmodified Co<sub>3</sub>O<sub>4</sub>, thanks to enhanced charge transfer dynamics and increased surface area. These comparisons underscore the superior efficiency and functionality of TMO/GO composites in CO<sub>2</sub> reduction applications over conventional single-phase photocatalysts.<sup>84–86</sup>

## 5. Energy storage applications

Apart from renewable energy conversion applications, transition metal oxide/graphene oxide (TMO/GO) composites have also been among the prospective next-generation energy storage devices due to their synergistic electrochemical performance. Energy storage is the backbone of contemporary energy systems that enables the secure integration of non-dispatchable renewable sources like solar and wind by retaining surplus energy to utilize it during periods of low generation or high demand.<sup>87</sup> Not only does this ability enhance grid stability and flexibility but also maximizes the harvesting of clean energy, reduces the consumption of fossil fuels, and makes possible the creation of a robust, sustainable energy system. Among the high-performance materials promoting development in this area are

transition metal oxide/graphene oxide (GO) nanocomposites with excellent electrochemical performance.<sup>88</sup> Transition metal oxides deposited on GO sheets lead to hybrid materials with high surface area, appropriate electrical conductivity, and mechanical strength, all of which are required for energy storage devices to perform well. These nanocomposites facilitate high rate charging and discharging operations, improve conductivity of the charge carriers, and provide the overall energy and power density of the storage device at the highest levels. These materials find the most valuable applications in devices such as lithium-ion batteries and supercapacitors where they optimize some inherent limitations with standard electrodes.<sup>88,89</sup>

As discussed above, TMOs combined with GO exhibit synergistic effects that enhance the electrochemical properties of energy storage devices. These composites demonstrate improved conductivity, charge storage, and stability compared to individual components.<sup>48,90</sup> Obodo *et al.* (2020)<sup>48</sup> has discussed the incorporation of GO in TMO nanocomposites, increases surface area and electrical conductivity, leading to higher specific capacitance and better electrode performance. *In situ* Raman Spectro electrochemistry reveals the dynamic processes at the graphene-TMO/electrolyte interface, providing insights into charge transfer mechanisms.<sup>91</sup> Nickel oxide/graphene composites, in particular, show promise for various electrochemical applications due to their cost-effectiveness and superior performance as shown by Liu *et al.* (2018).<sup>92</sup> The synergistic interactions between TMOs and GO result from ionic interactions, interface engineering, and the formation of chemically bridged interfaces with tunable properties.<sup>91</sup> Therefore, TMO/GO nanocomposites are critical to enabling next-generation energy storage devices required to balance renewable energy supply, support electric vehicles, and power portable electronics, hence being at the forefront of the world's shift to cleaner and more secure energy systems.<sup>93</sup>

### 5.1. Supercapacitors

Supercapacitors, also called ultracapacitors, are novel electrochemical energy storage systems midway between rechargeable batteries and conventional capacitors.<sup>94</sup> They are characterized by their very high capacitance and energy density because electrodes have large surface areas and very thin separators enable double layers of electrostatics and in some instances pseudo capacitance from redox materials.<sup>94</sup> As opposed to batteries, supercapacitors charge and discharge significantly faster, can withstand millions of charge–discharge cycles, and can maintain high power density, appropriate for application in applications that include rapid energy pulses, such as regenerative braking in vehicles, power backup systems, and grid stabilization.<sup>87</sup> The operation mechanism is attributed to ion adsorption at the electrode–electrolyte interface, thus providing quick charge storage and discharge with minimal degradation over time.<sup>87,94</sup>

The introduction of TMO nanoparticle additives, *e.g.*, Ni-doped ZnO, into graphene oxide GO films has significantly enhanced supercapacitor performance. GO provides a highly conductive two-dimensional network that facilitates rapid electron transfer, while its high surface area provides more ions



adsorption and electrode–electrolyte interface.<sup>94</sup> When combined with the electrochemical activity of TMOs like Ni–ZnO, which exhibit faradaic (redox) pseudo capacitance, the resulting nanocomposite electrodes exhibit both high specific capacitance and excellent cycling stability.<sup>87</sup> High conductivity of GO effectively suppresses charge recombination and resistance losses, while Ni–ZnO nanoparticles introduce additional redox-active sites, further increasing capacitance and enabling stable operation for thousands of cycles. This combination generates supercapacitors that are not only highly fast charging and discharging, but also, they can maintain good performance with increased use, and therefore TMO/GO composites are immensely helpful for energy storage technology of the future.<sup>79,94</sup>

Recent studies have demonstrated significant enhancement of supercapacitor performance through the incorporation of TMO nanoparticle additives into GO films. Gupta *et al.* (2024)<sup>91</sup> has discussed NiO/ZnO@GO nanocomposites have shown remarkable specific capacitance of 1833.9 F g<sup>-1</sup> and 98.7% capacity retention after 6000 cycles. Similarly, NiO–ZnO/GO binary metal oxide nanocomposites achieved a high specific capacitance of 1690 F g<sup>-1</sup> with excellent conductivity.<sup>91</sup> Monolayer graphene/NiO nanosheets exhibited a specific capacitance of 525 F g<sup>-1</sup> with 95.4% retention after 1000 cycles as indicated by Zhao *et al.* (2011).<sup>95</sup> Furthermore, Co<sub>3</sub>O<sub>4</sub>/MnO<sub>2</sub>/NiO/GO nanocomposites synthesized *via* chemical bath deposition demonstrated superior performance compared to single TMO electrodes, with specific capacitance values reaching 2482 F g<sup>-1</sup>.<sup>96</sup> These studies highlight the synergistic effects of TMO nanoparticles and GO in enhancing conductivity, surface area, and overall supercapacitor performance.

## 5.2. Lithium-ion batteries (LIBs)

Lithium-ion batteries (LIBs) dominate the rechargeable energy storage technology that is fueling a wide variety of applications from portable consumer electronics and electric vehicles to grid-scale energy storage systems. LIBs are the choice due to their precious energy and power density, high cycle life, low self-discharge rate, and low maintenance and hence being the pillar of mobility and energy requirements of the contemporary world.<sup>97</sup> The common composition of an LIB consists of

a graphite or other anode material, lithium metal oxide cathode, and liquid electrolyte which enables reversible intercalation and deintercalation of lithium ions between charge and discharge. Although ubiquitous in their presence, traditional LIBs suffer from some drawbacks: low specific capacity, capacity degradation upon repeated cycling, and the need for safer and more efficient electrode materials.<sup>97,98</sup>

Transition metal oxide/graphene oxide (TMO/GO) nanocomposites have been very promising anode materials in recent times to break through these drawbacks<sup>98</sup> TMOs such as NiO and ZnO exhibit far higher theoretical capacities for lithium storage than the conventional graphite but are compared with low electrical conductivity and significant volume expansion on cycling, which could lead to high-capacity fade.<sup>98</sup> The incorporation of such TMOs in GO sheets integrates graphene's excellent conductivity, mechanical flexibility, and massive surface area with metal oxide's high electrochemical activity to create electrochemically active electrodes with improved lithium-ion diffusion, structure stability, and excellent electrochemical performances. Specifically, Ni–ZnO/GO nanocomposite anodes provide many active sites for lithium storage, enable rapid electron and ion diffusion, and buffer TMO volume expansion during cycling to impart better reversible capacities and battery life.<sup>98,99</sup> The latest studies have proven that these composite metal oxide/GO materials are able to deliver significantly increased specific capacities and exhibit ideal cycling stability over thousands of cycles, even at high current densities, which makes them of extremely high value for next-generation high-performance LIBs.<sup>99</sup>

The process of designing each electrode starts with the use of active material powder, consisting of spherical or ellipsoidal particles ranging from nanometer to micrometer sizes. In the design, the powder is blended with conductive additives and binders, resulting in a mixture called porous electrode that maintains liquid filled pores. The structure contains the active material that forms the central component, selected to facilitate the battery's electrochemical reaction, generating electrical current while maintaining structural integrity during the intercalation and deintercalation of lithium ions. Lithium ions (Li<sup>+</sup>) are the primary charge-carrying entities in lithium-ion batteries, as depicted in Fig. 8.

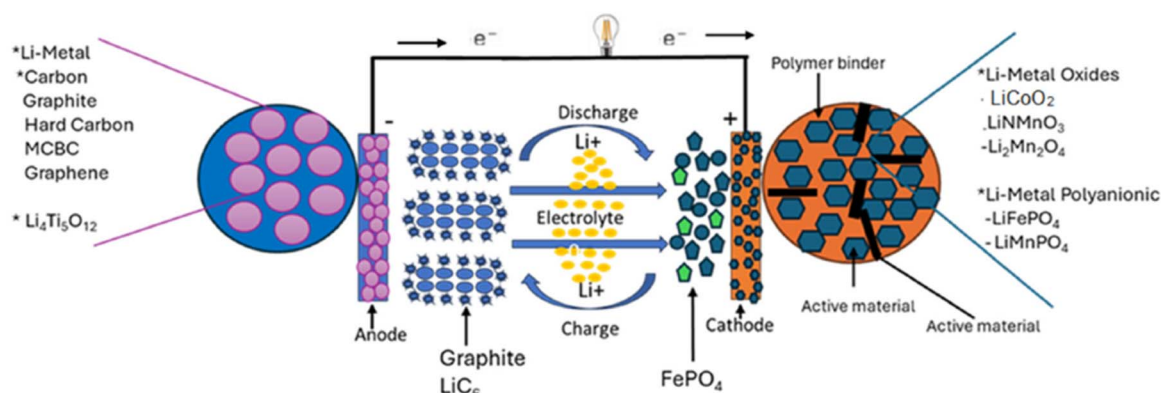


Fig. 8 Schematic diagram of basic components of an operational lithium-ion battery. (Reproduced from ref. 100 with permission from MDPI, copyright 2025).



Recent research has focused on improving TMO anodes for lithium-ion batteries by combining them with graphene-based materials. These composites exhibit enhanced electrical conductivity, structural stability, and electrochemical performance. Fe<sub>3</sub>O<sub>4</sub> microspheres encapsulated in graphene shells demonstrated high capacity and improved cycling performance as mentioned in Yu Jiang *et al.* (2015).<sup>101</sup> Fe<sub>2</sub>O<sub>3</sub>/MoO<sub>3</sub> quantum dots on N-doped graphene showed excellent rate capability and long-term stability due to strong covalent bonds and enhanced pseudo capacitance by Juan Ding *et al.* (2022).<sup>102</sup> A 3D porous Co<sub>3</sub>O<sub>4</sub>-CoO@GO composite with N-doped carbon displayed high capacity, superior rate performance, and excellent cycling stability.<sup>103</sup> These studies highlight the potential of TMO/GO composites as high-performance anodes for lithium-ion batteries. In the context of lithium-ion batteries, TMO/GO composites have shown remarkable improvements in electrochemical performance compared to their pristine counterparts. For example, Fe<sub>2</sub>O<sub>3</sub>/GO composites achieved a high specific capacity of 1053 mA h g<sup>-1</sup>, nearly three times greater than that of bare Fe<sub>2</sub>O<sub>3</sub>. This enhancement is largely due to graphene oxide's ability to buffer volume changes during charge-discharge cycles and to provide superior electrical conductivity. Similarly, NiCo<sub>2</sub>O<sub>4</sub>/GO electrodes delivered a capacity of 842 mA h g<sup>-1</sup>, more than double that of unmodified NiCo<sub>2</sub>O<sub>4</sub>. The presence of GO in the composite significantly improved cycling stability and charge transportation, making these hybrids highly promising candidates for next-generation energy storage systems.<sup>104,105</sup>

## 6. Challenges

### 6.1. Environmental concerns

Transition metal oxide/graphene-derived composite materials are multi-functional for catalytic dye degradation, renewable energy, and energy storage but with significant environmental impact issues. These involve ecotoxicity of TMOs such as NiO, ZnO, or MnO<sub>2</sub> that, upon leaching or improper disposal, add toxic metal ions to water and land environments that can damage microorganisms, plants, and organisms.<sup>106</sup> Their extreme reactivity and persistence can potentially exacerbate bioaccumulation and disrupt ecological balance, particularly when used at scale in water treatment or energy. In addition, graphene oxide environmental mobility is a risk with its nanoscale dimensions and surface functionalization, which has the potential for mobilizing through soil and water and, therefore, trigger unforeseen biological interactions and toxicity. Studies have revealed that GO can induce oxidative stress and membrane damage in aquatic organisms, which has raised concerns regarding its widespread use and release.<sup>106,107</sup>

The overall toxicity of the composite materials, especially that of TMOs and GO together, is finer than the single entities since they include synergistic interactions which would be able to augment biological activity or initiate new risks.<sup>108</sup> The illustration of an improved catalytic or electrocatalytic activity improving technological characteristics can also enhance in reactivity to biological molecules and induce increased cytotoxicity or genotoxicity. Moreover, the end-of-life phase also creates recycling and disposal problems: conventional waste

treatment processes cannot effectively recover or detoxify nanoscale materials, resulting in environmental persistence or secondary pollution.<sup>106,108</sup> There is no standardized process for the safe recycling or disposal of spent catalysts and used electrodes, so their sustainable deployment becomes challenging. Addressing these issues requires extensive lifecycle analysis, green synthesis and recovery operations, and legislation to reverse the environmental footprint of TMO/GO nanocomposites in actual usage.<sup>106,108</sup>

## 7. Future perspectives

The continuous advancement in graphene-based nanocomposite technologies presents significant potential for addressing emerging challenges in energy storage, environmental remediation, and catalysis. Notwithstanding notable progress, several critical avenues for future research remain open for exploration. One promising direction involves the strategic design and synthesis of mixed metal oxide/graphene oxide (GO) nanocomposites to optimize multifunctional performance.<sup>109</sup> Enhancing the structural integration and interfacial interactions between the components can significantly improve performance in energy storage devices, gas sensing, and photocatalytic systems. Specifically, research should focus on exploring less-studied transition metal oxides, such as TiO<sub>x</sub>, NiCoO<sub>x</sub>, and Co-MnO<sub>x</sub>, and their combination with graphene derivatives to improve catalytic activity in oxygen reduction reactions (ORR), while also ensuring economic viability.<sup>110</sup> In photocatalytic applications, heterogeneous nanostructures incorporating graphene oxide (GO) or functionalized derivatives have shown promise in degrading synthetic dyes and pollutants. The development of novel ternary and quaternary composites, especially those integrated with semiconductors like TiO<sub>2</sub>, ZnO, and V<sub>2</sub>O<sub>5</sub>, remains a valuable direction for enhancing light absorption, charge separation, and reactive species generation under visible light.<sup>111-113</sup> The functionalization of GO, either chemically or biologically, could provide new pathways for tailoring surface properties to target specific pollutants or catalytic reactions.<sup>113</sup>

Moreover, investigating the dimensionality of nanostructures, such as one-dimensional nanorods, two-dimensional sheets, and three-dimensional frameworks, could reveal performance-related structure-function relationships. These studies may contribute to enhanced dye degradation efficiencies.<sup>110</sup> A critical aspect often overlooked is the long-term stability and reusability of these composites under real-world conditions. Assessing environmental robustness and structural integrity after multiple operational cycles is essential to ensure the practical deployment of such materials in industrial and municipal wastewater treatment systems.<sup>114-116</sup> Investigations into the regeneration of spent photocatalysts or adsorbents will further support the development of sustainable technologies.<sup>117</sup>

Additionally, incorporating biopolymers such as chitosan into GO-based systems offers eco-friendly alternatives with promising adsorption and mechanical properties. Exploring such biodegradable hybrid materials can bridge the gap



between high performance and environmental safety.<sup>117</sup> In biomedical and antimicrobial applications, the antibacterial properties of GO-based composites remain largely unexplored. Understanding their mechanisms of interaction with microbial membranes could facilitate the design of new protective coatings and filtration systems.<sup>109</sup>

Lastly, the scalability and cost-effectiveness of synthesis methods, such as hydrothermal synthesis, sol-gel techniques, and green chemistry approaches, need further optimization. Industrial-scale implementation demands not only high efficiency but also process simplicity and economic viability.<sup>115,116</sup>

## 8. Conclusion

The review indicates that transition metal oxide/graphene oxide (TMO/GO) nanocomposites are a significant development in multifunctional materials for clean energy and pollution abatement, both from overcoming the inherent limitations of the individual components and creating new synergistic functionalities. Even though TMO has several limitations with the band gap, doping metals has the ability to reduce the band gap by introducing additional bands between the valence band and the conduction band. The most significant novelty is the potential of such composites to efficiently deliver high-performance photocatalytic degradation of persistent organic pollutants, high-fraction hydrogen evolution, and enhanced energy storage on the one side, and employing scalable, eco-friendly synthesis routes compatible with sustainability goals on the other. Coupling TMOs with graphene derivatives such as enables enhanced electron transfer, surface area, and charge separation resulting in stable activity even under the intricate real-world conditions exemplified by high rates of dye degradation and stable electrode performance in batteries and supercapacitors. Most notably, these materials are moving from laboratory-scale proof-of-concept to actual, practical, industrial use, enabled by advances in eco-friendly synthesis, recyclability, and lifecycle management. However, the review also acknowledges the future challenges such as environmental contamination, leaching of nanoparticles, and recycling at the end of life also as important areas of future research, which necessitate standardized durability tests, closed-loop recycling, and regulation. The future research efforts should aim towards rational design of ternary and quaternary nanocomposites, exploration of less explored TMOs, and integration of biopolymers or integration of support biodegradable to further push the performances, environmental compatibility, and scalability. Lastly, TMO/GO nanocomposites have the potential to be pillar materials in bringing the world's economies to circular and decarbonized economies, provided that interdisciplinary research goes on to make giant strides in synthesis, application, and sustainable lifecycle stewardship.

## Author contributions

Viraj Pasindu, Piumika Yapa, Sanduni Dabare – literature search and drafted the initial manuscript. Imalka Munaweera – conceptualization, supervision, writing, review and editing the

manuscript. All authors have given approval to the final version of the manuscript.

## Conflicts of interest

The authors declare that there is no conflict of interest.

## Data availability

No primary research results, software or code have been included, and no new data were generated or analyzed as part of this review.

## References

- 1 A. A. Firoozi, A. A. Firoozi, D. O. Oyejobi, S. Avudaiappan and E. S. Flores, Emerging trends in sustainable building materials: Technological innovations, enhanced performance, and future directions, *Results Eng.*, 2024, **24**, 103521. Available from: <https://www.sciencedirect.com/science/article/pii/S2590123024017729?via%3Dihub>.
- 2 A. Krishnan, A. Swarnalal, D. Das, M. Krishnan, V. S. Saji and S. M. A. Shibli, A review on transition metal oxides based photocatalysts for degradation of synthetic organic pollutants, *J. Environ. Sci.*, 2024, **139**, 389–417. Available from: <https://www.sciencedirect.com/science/article/abs/pii/S1001074223000979>.
- 3 X. R. Zhao, Y. Q. Cao, J. Chen, L. Zhu, X. Qian, A. D. Li, *et al.*, Photocatalytic Properties of Co<sub>3</sub>O<sub>4</sub>-Coated TiO<sub>2</sub> Powders Prepared by Plasma-Enhanced Atomic Layer Deposition, *Nanoscale Res. Lett.*, 2017, **12**, 497.
- 4 M. A. Ahmed, S. A. Mahmoud and A. A. Mohamed, Interfacially engineered metal oxide nanocomposites for enhanced photocatalytic degradation of pollutants and energy applications, *RSC Adv.*, 2025, **15**(20), 15561–15603.
- 5 D. Pradhan, K. Biswal susanta, N. Nayak, R. Singhal, S. K. Beriha and R. Pattanaik, *et al.*, Synergistic Photocatalytic and Supercapacitive Properties of Transition Metal Doped Co<sub>3</sub>O<sub>4</sub>: Towards Efficient Dye Degradation and Energy Storage, SSRN, 2024, pp. 8–10.
- 6 X. Chen, *et al.*, N-Butyllithium-Treated Ti<sub>3</sub>C<sub>2</sub>T<sub>x</sub> MXene with Excellent Pseudocapacitor Performance, *ACS Nano*, 2019, **13**(8), 9449–9456.
- 7 M. Cabello, G. F. Ortiz, P. Lavela and J. L. Tirado, On the Beneficial Effect of MgCl<sub>2</sub> as Electrolyte Additive to Improve the Electrochemical Performance of Li<sub>4</sub>Ti<sub>5</sub>O<sub>12</sub> as Cathode in Mg Batteries, *Nanomaterials*, 2019, **9**(3), 484.
- 8 F. Mashkoo, M. Shoeb, R. Mashkoo, A. H. Anwer, S. Zhu, H. Jeong, *et al.*, Synergistic effects of tungstate trioxide hemihydrate decorated reduced graphene oxide for the adsorption of heavy metals and dyes and postliminary application in supercapacitor device, *J. Clean. Prod.*, 2023, **418**, 138067.
- 9 T. G. Yun, *et al.*, Polypyrrole-MnO<sub>2</sub>-Coated Textile-Based Flexible-Stretchable Supercapacitor with High Electrochemical and Mechanical Reliability, *ACS Appl. Mater. Interfaces*, 2015, **7**(17), 9228–9234.





- 10 X. Li, D. Du, Y. Zhang, W. Xing, Q. Xue and Z. Yan, Layered double hydroxides toward high-performance supercapacitors, *J. Mater. Chem. A*, 2017, 5, 15460–15485.
- 11 X. Chen, R. Paul and L. Dai, Carbon-based supercapacitors for efficient energy storage, *Natl. Sci. Rev.*, 2017, 4(3), 453–489.
- 12 Z. Lei, F. Shi and L. Lu, Incorporation of MnO<sub>2</sub>-Coated Carbon Nanotubes between Graphene Sheets as Supercapacitor Electrode, *ACS Appl. Mater. Interfaces*, 2012, 4(2), 1058–1064.
- 13 V. Modafferi, S. Santangelo, M. Fiore, E. Fazio, C. Triolo, S. Patanè, *et al.*, Transition metal oxides on reduced graphene oxide nanocomposites: Evaluation of physicochemical properties, *J. Nanomater.*, 2019, 2019, 5–7.
- 14 W. Zhang, F. Liu, Q. Li, Q. Shou, J. Cheng, L. Zhang, *et al.*, Transition metal oxide and graphene nanocomposites for high-performance electrochemical capacitors, *Phys. Chem. Chem. Phys.*, 2012, 14(47), 16331–16337.
- 15 C. Bandas, C. Orha, M. Nicolaescu, M. I. Morariu Popescu and C. Lăzău, 2D and 3D Nanostructured Metal Oxide Composites as Promising Materials for Electrochemical Energy Storage Techniques: Synthesis Methods and Properties, *Int. J. Mol. Sci.*, 2024, 25(23), 12521.
- 16 D. Belotcerkovtceva, R. P. Maciel, E. Berggren, R. Maddu, T. Sarkar, Y. O. Kvashnin, *et al.*, Insights and Implications of Intricate Surface Charge Transfer and sp<sup>3</sup>-Defects in Graphene/Metal Oxide Interfaces, *ACS Appl. Mater. Interfaces*, 2022, 14(31), 36209–36216.
- 17 B. Anegebe, I. H. Ifijen, M. Maliki, I. E. Uwidia and A. I. Aigbodion, Graphene oxide synthesis and applications in emerging contaminant removal: a comprehensive review, *Environ. Sci. Eur.*, 2024, 36, 15.
- 18 V. S. Nazim, G. M. El-Sayed, S. M. Amer and A. H. Nadim, Optimization of metal dopant effect on ZnO nanoparticles for enhanced visible LED photocatalytic degradation of citalopram: comparative study and application to pharmaceutical cleaning validation, *Sustain. Environ. Res.*, 2023, 33(1), 39.
- 19 N. Madkhali, Analysis of Structural, Optical, and Magnetic Properties of (Fe,Co) Co-Doped ZnO Nanoparticles Synthesized under UV Light, *Condens. Matter*, 2022, 7(4), 63.
- 20 V. Shunaev and O. Glukhova, Interaction of Co<sub>3</sub>O<sub>4</sub> Nanocube with Graphene and Reduced Graphene Oxide: Adhesion and Quantum Capacitance, *Lubricants*, 2022, 10(5), 79.
- 21 J. Meyer, P. R. Kidambi, B. C. Bayer, C. Weijtens, A. Kuhn, A. Centeno, *et al.*, Metal Oxide Induced Charge Transfer Doping and Band Alignment of Graphene Electrodes for Efficient Organic Light Emitting Diodes, *Sci. Rep.*, 2014, 4(1), 5380.
- 22 B. Bhattacharyya, M. Geetha, H. Anwar, S. A. Zaidi, K. K. Sadasivuni, M. Mohamed, *et al.*, Synergistic Effect of TiO<sub>2</sub> Nanorods Incorporated with Graphene Oxide for Photocatalytic Degradation of Multiple Dyes, *Int. J. Environ. Res.*, 2025, 19(1), 34.
- 23 D. Ma, X. Mu, G. Zhao, X. Qin and M. Qi, MnO<sub>2</sub>/Carbon Nanofibers Material as High-Performance Anode for Lithium-Ion Batteries, *Coatings*, 2023, 13(4), 707.
- 24 R. Al-Tohamy, S. S. Ali, F. Li, K. M. Okasha, Y. A. G. Mahmoud, T. Elsamahy, *et al.*, A critical review on the treatment of dye-containing wastewater: Ecotoxicological and health concerns of textile dyes and possible remediation approaches for environmental safety, *Ecotoxicol. Environ. Saf.*, 2022, 231, 113160. Available from: <https://www.sciencedirect.com/science/article/pii/S0147651321012720>.
- 25 B. Lellis, C. Z. Fávoro-Polonio, J. A. Pamphile and J. C. Polonio, Effects of textile dyes on health and the environment and bioremediation potential of living organisms, *Biotechnol. Res. Innov.*, 2019, 3(2), 275–290. Available from: <https://www.sciencedirect.com/science/article/pii/S2452072119300413>.
- 26 H. Hassena, Photocatalytic Degradation of Methylene Blue by Using Al<sub>2</sub>O<sub>3</sub>/Fe<sub>2</sub>O<sub>3</sub> Nano Composite under Visible Light, *Mod. Chem. Appl.*, 2016, 5(9), 1–5.
- 27 K. Ranathunga, P. Yapa, I. Munaweera, M. M. Weerasekera and C. Sandaruwan, Preparation and characterization of Fe-ZnO cellulose-based nanofiber mats with self-sterilizing photocatalytic activity to enhance antibacterial applications under visible light, *RSC Adv.*, 2024, 14(26), 18536–18552.
- 28 X. Q. Wang, S. F. Han, Q. W. Zhang, N. Zhang and D. D. Zhao, Photocatalytic oxidation degradation mechanism study of methylene blue dye waste water with GR/iTO<sub>2</sub>, in *MATEC Web of Conferences*, EDP Sciences, 2018.
- 29 P. Ghasemipour, M. Fattahi, B. Rasekh and F. Yazdian, Developing the Ternary ZnO Doped MoS<sub>2</sub> Nanostructures Grafted on CNT and Reduced Graphene Oxide (RGO) for Photocatalytic Degradation of Aniline, *Sci. Rep.*, 2020, 10(1), 4414.
- 30 C. Vyas and M. Choudhary, *Degradation of methylene blue dye as wastewater pollutant by atmospheric pressure plasma: A comparative study*, 2023, DOI: [10.48550/arXiv.2301.11053](https://doi.org/10.48550/arXiv.2301.11053).
- 31 H. Salehzadeh, K. Wantala, E. Mohammadi, H. P. Shivaraju, B. Shahmoradi, S. Rtimi, A. Maleki and M. Safari, Solar photodegradation of malathion from aqueous media using Al-doped ZnO/Fe<sub>3</sub>O<sub>4</sub> nanocomposite, *Catal. Commun.*, 2023, 184, 106785.
- 32 J. Patel, R. N. Kumar and J. I. N. Kumar, A Comprehensive Review on Waste Water Treatment Technologies with Special Emphasize on Biological Treatments, *Int. J. Life Sci. Pharma Res.*, 2023, 13, L112–L124.
- 33 Y. Wu, B. Zeng, M. Guan, L. Han, X. Zhang and W. Ge, Enhancement of double heterojunction Bi<sub>12</sub>SiO<sub>20</sub>-Bi<sub>2</sub>O<sub>2</sub>SiO<sub>3</sub>-BiOX<sub>m</sub>Y<sub>n</sub> with high Adsorption-Visible catalytic Performance: Synergistic effect of morphology regulation and controllable energy band, *J. Mol. Liq.*, 2022, 348, 118065.
- 34 T. X. Huang, B. Dong, S. L. Filbrun, A. Ahmad Okmi, X. Cheng, M. Yang, *et al.*, Single-molecule photocatalytic dynamics at individual defects in two-dimensional layered materials, *Sci. Adv.*, 2021, 7(40), eabj4452.



- 35 S. Das, S. K. Dash and K. M. Parida, Kinetics, Isotherm, and Thermodynamic Study for Ultrafast Adsorption of Azo Dye by an Efficient Sorbent: Ternary Mg/(Al + Fe) Layered Double Hydroxides, *ACS Omega*, 2018, **3**(3), 2532–2545.
- 36 R. Ananthashankar, Effectiveness of photocatalytic decolourization of reactive red 120 dye in textile effluent using UV/H<sub>2</sub>O<sub>2</sub> Am, *J. Environ. Sci.*, 2013, **9**(4), 322–333.
- 37 A. D. Hewamadduma and T. K. Weerasinghe, Treatment Of Textile Effluent Containing Reactive Black 5 Dye Using Advanced Oxidation, *Int. J. Sci. Res. Eng. Dev.*, 2021, **4**(1), IJSRED-V411P5.
- 38 Y. S. Ma, C. N. Chang and C. R. Chao, Decolorization of Rhodamine B by a Photo-Fenton Process: Effect of System Parameters and Kinetic, *Int. J. Energy Sect. Manag.*, 2012, **1**(2), 73–80.
- 39 D. O. Idisi, C. C. Ahia, E. L. Meyer, J. O. Bodunrin and E. M. Benecha, Graphene oxide:Fe<sub>2</sub> O<sub>3</sub> nanocomposites for photodetector applications: experimental and *ab initio* density functional theory study, *RSC Adv.*, 2023, **13**(9), 6038–6050.
- 40 D. O. Idisi, C. C. Ahia, E. L. Meyer, J. O. Bodunrin and E. M. Benecha, Graphene oxide:Fe<sub>2</sub> O<sub>3</sub> nanocomposites for photodetector applications: experimental and *ab initio* density functional theory study, *RSC Adv.*, 2023, **13**(9), 6038–6050.
- 41 V. Shunaev and O. Glukhova, Interaction of Co<sub>3</sub>O<sub>4</sub> Nanocube with Graphene and Reduced Graphene Oxide: Adhesion and Quantum Capacitance, *Lubricants*, 2022, **10**(5), 79.
- 42 V. Shunaev and O. Glukhova, Interaction of Co<sub>3</sub>O<sub>4</sub> Nanocube with Graphene and Reduced Graphene Oxide: Adhesion and Quantum Capacitance, *Lubricants*, 2022, **10**(5), 79.
- 43 D. O. Idisi, C. C. Ahia, E. L. Meyer, J. O. Bodunrin and E. M. Benecha, Graphene oxide:Fe<sub>2</sub> O<sub>3</sub> nanocomposites for photodetector applications: experimental and *ab initio* density functional theory study, *RSC Adv.*, 2023, **13**(9), 6038–6050.
- 44 J. Luan, K. Ma, S. Wang, Z. Hu, Y. Li and B. Pan, Research on Photocatalytic Degradation Pathway and Degradation Mechanisms of Organics, *Curr. Org. Chem.*, 2010, **14**(7), 645–682.
- 45 G. Sriram, M. Arunpandian, K. Dhanabalan, V. R. Sarojamma, S. David, M. D. Kurkuri, *et al.*, Recent Progress Using Graphene Oxide and Its Composites for Supercapacitor Applications: A Review, *Inorganics*, 2024, **12**(6), 145.
- 46 G. K. Gupta and M. K. Mondal, Fundamentals and mechanistic pathways of dye degradation using photocatalysts, in *Photocatalytic Degradation of Dyes*, Elsevier, 2021, pp. 527–545.
- 47 M. M. Almutairi, E. E. Ebraheim, M. S. Mahmoud, M. S. Atrees, M. E. M. Ali and Y. M. Khawassek, Nanocomposite of TiO<sub>2</sub> @ Ni- or Co-doped graphene oxide for efficient photocatalytic water splitting, *Egypt. J. Chem.*, 2019, **62**(9), 1649–1658.
- 48 R. M. Obodo, E. O. Onah, H. E. Nsude, A. Agbogu, A. C. Nwanya, I. Ahmad, *et al.*, Performance Evaluation of Graphene Oxide Based Co<sub>3</sub> O<sub>4</sub> @GO, MnO<sub>2</sub> @GO and Co<sub>3</sub> O<sub>4</sub>/MnO<sub>2</sub> @GO Electrodes for Supercapacitors, *Electroanalysis*, 2020, **32**(12), 2786–2794.
- 49 S. Sasidharan, S. V. Sasidharan Nair, A. Sudhakaran and R. Sreenivasan, Insight into the Fabrication and Characterization of Novel Heterojunctions of Fe<sub>2</sub> O<sub>3</sub> and V<sub>2</sub> O<sub>5</sub> with TiO<sub>2</sub> and Graphene Oxide for Enhanced Photocatalytic Hydrogen Evolution: A Comparison Study, *Ind. Eng. Chem. Res.*, 2022, **61**(7), 2714–2733.
- 50 P. Bernard, P. Stelmachowski, P. Broś, W. Makowski and A. Kotarba, Demonstration of the Influence of Specific Surface Area on Reaction Rate in Heterogeneous Catalysis, *J. Chem. Educ.*, 2021, **98**, 935–940.
- 51 C. C. Wang and J. Y. Ying, Sol–Gel Synthesis and Hydrothermal Processing of Anatase and Rutile Titania Nanocrystals, *Chem. Mater.*, 1999, **11**(11), 3113–3120.
- 52 A. Haleem, M. Ullah, S. Rehman, A. Shah, M. Farooq, T. Saeed, *et al.*, In-Depth Photocatalytic Degradation Mechanism of the Extensively Used Dyes Malachite Green, Methylene Blue, Congo Red, and Rhodamine B via Covalent Organic Framework-Based Photocatalysts, *Water*, 2024, **16**(11), 1588.
- 53 M. M. Islam, I. Tateishi, M. Furukawa, H. Katsumata, T. Suzuki and S. Kaneco, Evaluation of Reaction Mechanism for Photocatalytic Degradation of Dye with Self-Sensitized TiO<sub>2</sub> under Visible Light Irradiation, *Open J. Inorg. Non-Metallic Mater.*, 2017, **07**(01), 1–7.
- 54 F. Bi, Q. Meng, Y. Zhang, X. Weng and Z. Wu, Defect Engineering in 0D/2D S-Scheme Heterojunction Photocatalysts for Water Activation: Synergistic Roles of Nickel Doping and Oxygen Vacancy, *ACS Appl. Mater. Interfaces*, 2023, **15**(26), 31409–31420.
- 55 C. Sanchez Tobon, I. Panžić, A. Bafti, G. Matijašić, D. Ljubas and L. Lidija Ćurković, Rapid Microwave-Assisted Synthesis of N/TiO<sub>2</sub>/rGO Nanoparticles for the Photocatalytic Degradation of Pharmaceuticals, *Nanomaterials*, 2022, **12**, 3975.
- 56 J. Di, G. Hao, W. Jiang and Z. Liu, Defect Chemistry in 2D Atomic Layers for Energy Photocatalysis, *Acc. Mater. Res.*, 2023, **4**(11), 910–924.
- 57 J. Di, G. Hao, W. Jiang and Z. Liu, Defect Chemistry in 2D Atomic Layers for Energy Photocatalysis, *Acc. Mater. Res.*, 2023, **4**(11), 910–924.
- 58 D. Pradhan, S. K. Biswal, N. Nayak, R. Singhal, S. K. Beriha, R. Pattanaik, *et al.*, Bioinspired Synthesis of Transition Metal-Enhanced Co<sub>3</sub>O<sub>4</sub> Using *Mangifera indica* Leaves for Photocatalytic and Energy Storage Applications, *ChemistrySelect*, 2024, **9**(48), e202403211.
- 59 S. Soren, S. Chakraborty and K. Pal, Enhanced in tuning of photochemical and electrochemical responses of inorganic metal oxide nanoparticles via rGO frameworks (MO/rGO): A comprehensive review, *Mater. Sci. Eng., B*, 2022, **278**, 115632.
- 60 M. Lu, H. Li, S. Li, F. Yang, Y. Cao and W. Qiu, A study of the synergetic effect between graphene oxide and transition



- metal oxides for energy storage, *Sustain. Energy Fuels*, 2022, **6**(14), 3453–3464.
- 61 R. J. Toh, H. L. Poh, Z. Sofer and M. Pumera, Transition Metal (Mn, Fe, Co, Ni)-Doped Graphene Hybrids for Electrocatalysis, *Chem. Asian J.*, 2013, **8**(6), 1295–1300.
- 62 J. Zhu, T. Zhu, X. Zhou, Y. Zhang, X. W. Lou, X. Chen, *et al.*, Facile synthesis of metal oxide/reduced graphene oxide hybrids with high lithium storage capacity and stable cyclability, *Nanoscale*, 2011, **3**(3), 1084–1089.
- 63 M. Kobielsuz, A. Nitta, W. MacYk and B. Ohtani, Combined Spectroscopic Methods of Determination of Density of Electronic States: Comparative Analysis of Diffuse Reflectance Spectroelectrochemistry and Reversed Double-Beam Photoacoustic Spectroscopy, *J. Phys. Chem. Lett.*, 2021, **12**(11), 3019–3025.
- 64 Z. A. Sandhu, M. A. Raza, A. F. Kainat, M. S. Arshid, S. D. Kashf Jaffary, *et al.*, Graphene-Metal oxide Nanocomposites: Empowering Next-Generation energy storage devices, *Mater. Sci. Eng., B*, 2025, **313**, 117947. Available from: <https://www.sciencedirect.com/science/article/abs/pii/S0921510724007761>.
- 65 S. Y. Tee, K. Y. Win, W. S. Teo, L. D. Koh, S. Liu, C. P. Teng, *et al.*, Recent Progress in Energy-Driven Water Splitting, *Adv. Sci.*, 2017, **4**(5), 1600337.
- 66 L. Xiao, S. Y. Wu and Y. R. Li, Advances in solar hydrogen production via two-step water-splitting thermochemical cycles based on metal redox reactions, *Renew. Energy*, 2012, **41**, 1–12.
- 67 S. Sreekantan, K. A. Saharudin, N. Basiron and L. C. Wei, New-generation titania-based catalysts for photocatalytic hydrogen generation, *Nanostructured, Functional, and Flexible Materials for Energy Conversion and Storage Systems*, 2020, pp. 257–292.
- 68 A. K. Agegnehu, C. J. Pan, J. Rick, J. F. Lee, W. N. Su and B. J. Hwang, Enhanced hydrogen generation by cocatalytic Ni and NiO nanoparticles loaded on graphene oxide sheets, *J. Mater. Chem.*, 2012, **22**(27), 13849.
- 69 C. Wang, R. Ciganda, L. Yate, J. Tuninetti, V. Shalabaeva, L. Salmon, *et al.*, Redox synthesis and high catalytic efficiency of transition-metal nanoparticle–graphene oxide nanocomposites, *J. Mater. Chem. A*, 2017, **5**(41), 21947–21954.
- 70 A. K. Agegnehu, C. J. Pan, J. Rick, J. F. Lee, W. N. Su and B. J. Hwang, Enhanced hydrogen generation by cocatalytic Ni and NiO nanoparticles loaded on graphene oxide sheets, *J. Mater. Chem.*, 2012, **22**(27), 13849.
- 71 S. Sasidharan, S. V. Sasidharan Nair, A. Sudhakaran and R. Sreenivasan, Insight into the Fabrication and Characterization of Novel Heterojunctions of Fe<sub>2</sub>O<sub>3</sub> and V<sub>2</sub>O<sub>5</sub> with TiO<sub>2</sub> and Graphene Oxide for Enhanced Photocatalytic Hydrogen Evolution: A Comparison Study, *Ind. Eng. Chem. Res.*, 2022, **61**(7), 2714–2733.
- 72 E. Serrano, G. Rus and J. Garcia-Martínez, Nanotechnology for sustainable energy, *Renew. Sustain. Energy Rev.*, 2009, **13**(9), 2373–2384.
- 73 K. Sharma, V. Sharma and S. S. Sharma, Dye-Sensitized Solar Cells: Fundamentals and Current Status, *Nanoscale Res. Lett.*, 2018, **13**, 381.
- 74 F. T. Kong, S. Y. Dai and K. J. Wang, Review of recent progress in dye-sensitized solar cells, *Adv. Optoelectron.*, 2007, 75384.
- 75 C. A. Bignozzi, R. Argazzi, R. Boaretto, E. Busatto, S. Carli, F. Ronconi, *et al.*, The role of transition metal complexes in dye sensitized solar devices, *Coord. Chem. Rev.*, 2013, **257**(9–10), 1472–1492. Available from: <https://www.sciencedirect.com/science/article/abs/pii/S0010854512002342>.
- 76 C. L. T. Dang, C. Van Le, N. T. T. Le, M. T. T. Nguyen, D. C. Tran, K. T. Pham, *et al.*, Synthesis of titanium dioxide/reduced graphene oxide nanocomposite material via the incorporated hydrothermal co-precipitation method for fabricating photoanode in dye-sensitized solar cell, *Synth. Met.*, 2021, **281**, 116919.
- 77 A. C. Celline, A. Y. Subagja, S. Suryaningsih, A. Aprilia and L. Safriani, Synthesis of TiO<sub>2</sub>-rGO Nanocomposite and its Application as Photoanode of Dye-Sensitized Solar Cell (DSSC), *Mater. Sci. Forum*, 2021, **1028**, 151–156.
- 78 T. Shanmugapriya and J. Balavijayalakshmi, Role of graphene oxide/yttrium oxide nanocomposites as a cathode material for natural dye-sensitized solar cell applications, *Asia-Pac. J. Chem. Eng.*, 2021, **16**(2), e2598.
- 79 J. Zhang, M. Gu and X. Chen, Supercapacitors for renewable energy applications: A review, *Micro Nano Eng.*, 2023, **21**, 100229. Available from: <https://www.sciencedirect.com/science/article/pii/S259000722300059X>.
- 80 Y. Areeerob, C. Hamontree, P. Sricharoen, N. Limchoowong, S. Nijpanich, T. Nachaithong, W. Oh and K. Pattarith, Synthesis of novel MoWO<sub>4</sub> with ZnO nanoflowers on multi-walled carbon nanotubes for counter electrode application in dye-sensitized solar cells, *Sci. Rep.*, 2022, **12**, 12490.
- 81 W. Jiang, H. Loh, B. Q. L. Low, H. Zhu, J. Low, J. Z. X. Heng, *et al.*, Role of oxygen vacancy in metal oxides for photocatalytic CO<sub>2</sub> reduction, *Appl. Catal., B*, 2023, **321**, 122079. Available from: <https://www.sciencedirect.com/science/article/abs/pii/S0926337322010207>.
- 82 T. F. Yeh, J. Cihlář, C. Y. Chang, C. Cheng and H. Teng, Roles of graphene oxide in photocatalytic water splitting, *Mater. Today*, 2013, **16**(3), 78–84. Available from: <https://www.sciencedirect.com/science/article/pii/S1369702113000539>.
- 83 X. Li, J. Xiong, Z. Tang, W. He, Y. Wang, X. Wang, *et al.*, Recent Progress in Metal Oxide-Based Photocatalysts for CO<sub>2</sub> Reduction to Solar Fuels: A Review, *Molecules*, 2023, **28**(4), 1653.
- 84 D. Bu, D. Bu, W. Chen, C. Huang, L. Li, H. Lei, *et al.*, Metal-organic frameworks with mixed-anion secondary building units as efficient photocatalysts for hydrogen generation, *J. Catal.*, 2022, **407**, 10–18.
- 85 F. Pan, W. Deng, C. Justiniano and Y. Li, Identification of champion transition metals centers in metal and nitrogen-codoped carbon catalysts for CO<sub>2</sub> reduction, *Appl. Catal., B*, 2018, **226**, 463–472.
- 86 X. Lu, T. Yu, H. Wang, L. Qian and P. Lei, Electrochemical Fabrication and Reactivation of Nanoporous Gold with





- Abundant Surface Steps for CO<sub>2</sub> Reduction, *ACS Catal.*, 2020, **10**(15), 8860–8869.
- 87 B. Zhu, L. Fan, N. Mushtaq, R. Raza, M. Sajid, Y. Wu, *et al.*, Semiconductor Electrochemistry for Clean Energy Conversion and Storage, *Electrochem. Energy Rev.*, 2021, **4**, 757–792.
- 88 A. S. Ould, D. Rekioua, T. Rekioua and S. Bacha, Overview of energy storage in renewable energy systems, *Int. J. Hydrogen Energy*, 2016, **41**(45), 20914–20927. Available from: <https://www.sciencedirect.com/science/article/abs/pii/S0360319916309478>.
- 89 H. Kumagai, Y. Tamaki and O. Ishitani, Photocatalytic Systems for CO<sub>2</sub> Reduction: Metal-Complex Photocatalysts and Their Hybrids with Photofunctional Solid Materials, *Acc. Chem. Res.*, 2022, **55**(7), 978–990.
- 90 G. Tatrari, M. Ahmed and F. U. Shah, Synthesis, thermoelectric and energy storage performance of transition metal oxides composites, *Coord. Chem. Rev.*, 2024, **498**, 215470.
- 91 S. Gupta, S. B. Carrizosa, J. Jasinski and N. Dimakis, Charge transfer dynamical processes at graphene-transition metal oxides/electrolyte interface for energy storage: Insights from in-situ Raman spectroelectrochemistry, *AIP Adv.*, 2018, **8**(6), 065225.
- 92 Y. Liu, C. Gao, Q. Li and H. Pang, Nickel Oxide/Graphene Composites: Synthesis and Applications, *Chem.–Eur. J.*, 2019, **25**(9), 2141–2160.
- 93 I. Kamaraj and S. Kamaraj, in *Introduction to Energy Storage and Conversion*, 2024, pp. 1–27, DOI: [10.1021/bk-2024-1477.ch001](https://doi.org/10.1021/bk-2024-1477.ch001).
- 94 J. Libich, J. Máca, J. Vondrák, O. Čech and M. Sedlářková, Supercapacitors: Properties and applications, *J. Energy Storage*, 2018, **17**, 224–227.
- 95 B. Zhao, J. Song, P. Liu, W. Xu, T. Fang, Z. Jiao, *et al.*, Monolayer graphene/NiO nanosheets with two-dimension structure for supercapacitors, *J. Mater. Chem.*, 2011, **21**(46), 18792.
- 96 A. Alshoibi, C. Awada, N. Alnaim, N. Almulhem, R. M. Obodo, M. Maaza, *et al.*, Investigation of Chemical Bath Deposited Transition Metals/GO Nanocomposites for Supercapacitive Electrodes, *Crystals*, 2022, **12**(11), 1613.
- 97 Y. Mishra, A. Chattaraj, A. A. Aljabali, M. El-Tanani, M. M. Tambuwala and V. Mishra, Graphene oxide–lithium-ion batteries: inauguration of an era in energy storage technology, *Clean Energy*, 2024, **8**, 194–205.
- 98 H. Su, S. Jaffer and H. Yu, Transition metal oxides for sodium-ion batteries, *Energy Storage Mater.*, 2016, **5**, 116–131. Available from: <https://www.sciencedirect.com/science/article/abs/pii/S2405829716301374>.
- 99 K. Ullah, N. Shah, R. Wadood, B. M. Khan and W. C. Oh, Recent trends in graphene based transition metal oxides as anode materials for rechargeable lithium-ion batteries, *Nano Trends*, 2023, **1**, 100004. Available from: <https://www.sciencedirect.com/science/article/pii/S2666978123000016>.
- 100 I. B. Mansir and P. C. Okonkwo, Component Degradation in Lithium-Ion Batteries and Their Sustainability: A Concise Overview, *Sustainability*, 2025, **17**(3), 1000.
- 101 Y. Jiang, Z. J. Jiang, L. Yang, S. Cheng and M. Liu, A high-performance anode for lithium ion batteries: Fe<sub>3</sub>O<sub>4</sub> microspheres encapsulated in hollow graphene shells, *J. Mater. Chem. A*, 2015, **3**(22), 11847–11856.
- 102 J. Ding, R. Sheng, Y. Zhang, Y. Huang, W. Cheng, Z. Liu, *et al.*, Fe<sub>2</sub>O<sub>3</sub>/MoO<sub>3</sub>@NG Heterostructure Enables High Pseudocapacitance and Fast Electrochemical Reaction Kinetics for Lithium-Ion Batteries, *ACS Appl. Mater. Interfaces*, 2022, **14**(33), 37747–37758.
- 103 Y. Xu, C. Wu, L. Ao, K. Jiang, L. Shang, Y. Li, *et al.*, Three-dimensional porous Co<sub>3</sub>O<sub>4</sub>-CoO@GO composite combined with N-doped carbon for superior lithium storage, *Nanotechnology*, 2019, **30**(42), 425404.
- 104 S. Savithri, P. Remya, S. Vanitharaj, S. Selvakumar, P. Krishnan, S. Sudharthini, *et al.*, Hydrothermal synthesis of NiCo<sub>2</sub>O<sub>4</sub> Nanorods: A promising electrode material for supercapacitors with enhanced capacitance and stability, *Chem. Phys. Lett.*, 2025, **869**, 142028. Available from: <https://www.sciencedirect.com/science/article/abs/pii/S000926142500168X>.
- 105 X. Chen, Y. Zeng, Z. Chen, S. Wang, C. Xin, L. Wang, *et al.*, Synthesis and Electrochemical Property of FeOOH/Graphene Oxide Composites, *Front. Chem.*, 2020, **8**, 328.
- 106 P. Zare, M. Aleemardani, A. Seifalian, Z. Bagher and A. M. Seifalian, Graphene oxide: Opportunities and challenges in biomedicine, *Nanomaterials*, 2021, **11**, 1083.
- 107 S. Mandal, S. Mallapur, M. Reddy, J. K. Singh, D. E. Lee and T. Park, An Overview on Graphene-Metal Oxide Semiconductor Nanocomposite: A Promising Platform for Visible Light Photocatalytic Activity for the Treatment of Various Pollutants in Aqueous Medium, *Molecules*, 2020, **25**, 5380.
- 108 D. Malavekar, D. Pawar, A. Bagde, S. Khot, S. Sankapal, S. Bachankar, *et al.*, Advancements in graphene and its derivatives based composite Materials: A comprehensive review on Synthesis, Characterization, and supercapacitive charge storage, *Chem. Eng. J.*, 2024, **501**, 157533. Available from: <https://www.sciencedirect.com/science/article/abs/pii/S1385894724090247>.
- 109 R. Sharma, H. Kumar, D. Yadav, C. Saini, R. Kumari, G. Kumar, *et al.*, Synergistic advancements in nanocomposite design: Harnessing the potential of mixed metal oxide/reduced graphene oxide nanocomposites for multifunctional applications, *J. Energy Storage*, 2024, **93**, 112317.
- 110 M. Sun, H. Liu, Y. Liu, J. Qu and J. Li, Graphene-based transition metal oxide nanocomposites for the oxygen reduction reaction, *Nanoscale*, 2015, **7**(4), 1250–1269.
- 111 F. Jafari and F. R. Rahsepar, V<sub>2</sub>O<sub>5</sub>-Fe<sub>3</sub>O<sub>4</sub>/rGO Ternary Nanocomposite with Dual Applications as a Dye Degradation Photocatalyst and OER Electrocatalyst, *ACS Omega*, 2023, **8**(38), 35427–35439.
- 112 J. Campos-Delgado and M. E. Mendoza, Ternary Graphene Oxide and Titania Nanoparticles-Based Nanocomposites





- for Dye Photocatalytic Degradation: A Review, *Materials*, 2023, **17**(1), 135.
- 113 R. Sharma, H. Kumar, D. Yadav, C. Saini, R. Kumari, G. Kumar, *et al.*, Synergistic advancements in nanocomposite design: Harnessing the potential of mixed metal oxide/reduced graphene oxide nanocomposites for multifunctional applications, *J. Energy Storage*, 2024, **93**, 112317.
- 114 P. K. Boruah, P. Borthakur, G. Darabdhara, C. K. Kamaja, I. Karbhal, M. V. Shelke, *et al.*, Sunlight assisted degradation of dye molecules and reduction of toxic Cr(VI) in aqueous medium using magnetically recoverable Fe<sub>3</sub>O<sub>4</sub>/reduced graphene oxide nanocomposite, *RSC Adv.*, 2016, **6**(13), 11049–11063.
- 115 S. Mahalingam, J. Ramasamy and Y. H. Ahn, Enhanced Photocatalytic Degradation of Synthetic Dyes and Industrial Dye Wastewater by Hydrothermally Synthesized G-CuO-Co<sub>3</sub>O<sub>4</sub> Hybrid Nanocomposites Under Visible Light Irradiation, *J. Cluster Sci.*, 2018, **29**(2), 235–250.
- 116 A. A. Wani, R. A. Rather, N. Shaari, U. Khan, T. Muhammad, S. M. Hussain, *et al.*, Aspects of superior photocatalytic dye degradation and adsorption efficiency of reduced graphene oxide multiwalled carbon nanotubes with modified ZnO-Al<sub>2</sub>O<sub>3</sub> nanocomposites, *J. Environ. Chem. Eng.*, 2024, **12**(2), 112461.
- 117 R. Rajendiran, A. Patchaiyappan, S. Harisingh, P. Balla, A. Paari, B. Ponnala, *et al.*, Synergistic effects of graphene oxide grafted chitosan & decorated MnO<sub>2</sub> nanorods composite materials application in efficient removal of toxic industrial dyes, *J. Water Proc. Eng.*, 2022, **47**, 102704.

